PERGAMON

Journal of the Mechanics and Physics of Solids
50 (2002) 283–320

JOURNAL OF THE
MECHANICS AND
PHYSICS OF SOLIDS

www.elsevier.com/locate/jmps

A constrained theory of magnetoelasticity

Antonio DeSimone[a], Richard D. James[b, *]

[a] *Max Planck Institute for Mathematics in the Sciences, 04103 Leipzig, Germany*
[b] *Department of Aerospace Engineering and Mechanics, University of Minnesota, 107 Akerman Hall, 110 Union Street, Minneapolis, MN 55455, USA*

Received 28 November 2000; received in revised form 22 March 2001; accepted 22 March 2001

Abstract

A simple variational theory for the macroscopic behavior of materials with high anisotropy is derived rigorously from micromagnetics. The derivation leads to a constrained theory in which the state of strain and magnetization lies very near the 'energy wells' on most of the body. When specialized to ellipsoidal specimens and constant applied field and stress, the theory becomes a finite dimensional quadratic programming problem. Streamlined methods for solving this problem are given. The theory is illustrated by a prediction of the magnetoelastic behavior of the giant magnetostrictive material $Tb_{0.3}Dy_{0.7}Fe_2$. The theory embodies precisely the assumptions that have been postulated for ideal ferromagnetic shape memory, in which the magnetization stays rigidly attached to the easy axes of a martensitic material in the martensitic phase. More generally, the framework can be viewed as a prototype for the derivation of constrained theories for materials that change phase, and whose free-energy density grows steeply away from its minima.

Keywords: A. Microstructures; B. Magnetoelastic material; C. Energy methods

1. Introduction

Magnetoelastic (or magnetostrictive) solids are those in which reversible deformations can be induced by an applied magnetic field. Typical configurations of magnetoelastic bodies under no applied field contain domains on which the strain and magnetization is approximately constant. Such domain patterns arise from the interaction of crystallography (because of the existence of preferred crystallographic directions: the easy axes of magnetization) with long-range dipolar effects (which disfavor configurations with uniform magnetization throughout the specimen). Upon application of a

* Corresponding author. Tel.: +1-612-625-706; fax: +1-612-626-1558.
E-mail addresses: desimone@mis.mpg.de (A. DeSimone), james@aem.umn.edu (R.D. James).

0022-5096/02/$ - see front matter
PII: S0022-5096(01)00050-3

field, there is a redistribution of the domains caused by the fact that certain easy axes are more favorably oriented towards the applied field. Since domains with different magnetization also have different strains, this cooperative redistribution also leads to a macroscopic strain. As the field is further increased, substantial rotation of the magnetization within domains occurs and this causes a further contribution to the macroscopic strain. This paper is primarily concerned with the first part of the process.

Magnetostriction is typically a small effect, 20–200 microstrain in Fe, Ni and Co alloys. However, giant magnetostrictive materials, developed by Clark and his co-workers in the 1970s, have strains of the order of 10^{-3}. Among these, the alloy $Tb_{0.3}Dy_{0.7}Fe_2$ has enjoyed the greatest commercial success as an actuator material (Clark, 1992).

More recently, a new concept of magnetostriction has emerged, termed ferromagnetic shape memory (James and Wuttig, 1996), see also Tickle et al. (1999) and Ullakko et al. (1996). Ferromagnetic shape memory materials such as Ni_2MnGa or Fe_3Pd undergo a reversible first-order martensitic phase transformation upon cooling, and are also ferromagnetic. The crystallography of twinning implies that neighboring variants have nearly perpendicular easy axes, and therefore, the specimen can be biased toward one variant or another by applying a magnetic field. Because the transformation is first order, unlike in ordinary or giant magnetostrictive materials in which the ferromagnetic transition is second order, very large strains can be produced by variant redistribution. Reversible field-induced strains some 50 times those of giant magnetostrictive materials have been produced by this method (Tickle and James, 1999) in the alloy $Ni_{51.3}Mn_{24.0}Ga_{24.7}$ under modest fields. There are two material properties that are particularly important for ferromagnetic shape memory: mobile twin boundaries and high magnetic anisotropy (James and Wuttig, 1996). The latter is crucial because high magnetic anisotropy implies that the magnetization stays rigidly attached to the easy axes even as the field is increased. This ensures a significant driving force on the twin boundaries.

A well-established variational model, called Micromagnetics (Brown, 1963, 1966), is in principle available to describe the magnetomechanical response of magnetostrictive solids. The general micromagnetic problem for reasonably large samples is, however, difficult. That is because of the necessity of resolving exceedingly complex three-dimensional domain structures. The state-of-the-art in micromagnetic computations is 5–10 domains in a thin film (which effectively renders the computation two dimensional), and this in the purely magnetic case (no magnetostriction). Even in such computations, vortices that are thought to be present within domain walls are sometimes not resolved. Nevertheless, such computations have been extremely useful in science, engineering and industry. Typical mm scale specimens of ferromagnetic shape material that have been examined by magnetic force microscopy (Qi Pan and James, 2000) contain millions of domains just on the polished surface being observed. It seems utterly hopeless to think of doing a blind micromagnetic computation for a bulk ferromagnetic shape memory material, even if a reliable expression for the free-energy density valid for strains and magnetizations far from the energy wells were available, which it is not.

For this reason it is appealing to try to make use of the special features of some magnetostrictive and ferromagnetic shape memory materials to simplify the general micromagnetic problem. We do this in two ways. First (see Section 2), we make use

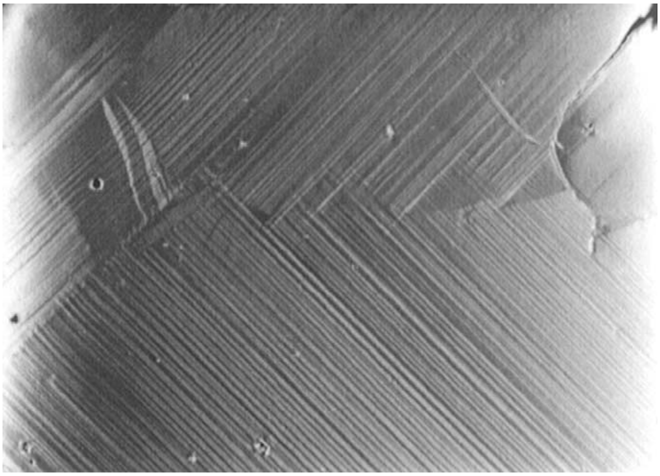

Fig. 1. Twinned elastic domains in the magnetic shape-memory alloy Ni_2MnGa. In the central portion of the picture, two layered domain structures meet through a horizontal transition layer. Detwinning occurs upon the application of a horizontal magnetic field. Picture frame is approximately 2.0×1.2 mm. Specimen courtesy of V.V. Kokorin, Ukrainian Academy of Sciences, micrograph courtesy of Rob Tickle, University of Minesota.

of the large body limit, as is done in the purely magnetic case by DeSimone (1993). This is equivalent to neglecting exchange energy and then studying the minimizing sequences of the total energy. Second (see Section 3), we study the limit of high anisotropy. This is done by examining the properties of a minimizer (or minimizing sequence) of the energy as the anisotropy constants tend to infinity. This has the effect of imposing a large energetic penalty to a (strain, magnetization) pair that does not lie on the energy wells. At first one might think that the effect of this would be to introduce a constraint that each (strain, magnetization) in the body must lie on the energy wells, but a rigorous analysis shows that the constraint is slightly weaker. (Precisely, it is that the Young measure of the sequence of these pairs is supported on the energy wells.) In fact the distinction is important: it is essential to allow for the possibility of narrow transition layers, of vanishingly small volume, where the (strain, magnetization) does not lie on the energy wells. Fig. 1 gives a pictorial illustration of such transition layers, while the precise formulation of the constraints is given in Section 3.

To exploit the resulting constrained theory, in Section 4 we take the viewpoint of relaxation. That is, we look for a simplified variational principle that governs the local average strain and local average magnetization. These local averages are sufficient to calculate the usual macroscopic magnetoelastic properties: magnetization curves and strain vs. field. The relaxed variational principle is summarized in Section 4.3. When it is further specialized to a constant applied field, constant applied stress and ellipsoidal body, the variational principle is drastically simplified. In particular, *the relaxed energy depends only on the values of a finite set of scalars $\theta_1, \dots, \theta_k$, where θ_i is the volume fraction of the specimen in which the state variables lie in the ith energy well*. The crucial fact which enables us to derive the simplified theory is that *every convex* *combination of* (*strain*, *magnetization*) *from an energy well represents a macroscopic state admissible within the constrained theory*. This is proved by direct construction of an associated microscopic state (Theorem 4.1). The main difficulty in these arguments is estimating the limiting behavior of the nonlocal magnetostatic energy.

In Section 5, we discuss some applications of our relaxed theory. It is remarkably easy to use, especially after an elementary change of variables and some simple observations about the resulting quadratic programming problem. We illustrate this by studying the magnetomechanical behavior of $Tb_{0.3}Dy_{0.7}Fe_2$.

Our constrained theory has also been applied to model the ferromagnetic shape memory alloys Ni_2MnGa and Fe_3Pd in various tests involving applied fields and applied stress. [1] Detailed comparisons with the corresponding experiments are given in Tickle et al. (1999), James and Wuttig (1998), and Tickle and James (1999). In the latter, comparisons between theory and experiment led the authors to propose that the easy axes of the FCT phase of $Fe_{70}Pd_{30}$ are the a-axis, in apparent disagreement with the results of calculations using density functional theory with spin (which suggest the c-axis is easy); recent measurements (Cui and James, 2000) of magnetization curves of $Fe_{70}Pd_{30}$ on detwinned specimens have confirmed that the a-axis are in fact the easy axes. Further examples where ideas similar to the ones discussed here are exploited are studies of hysteresis in martensites (Ball et al., 1995), and models for ferroelectric materials (Bhattacharya, 2000). Thus, the framework we present in this paper can be viewed as a prototype for the derivation of constrained theories for materials that change phase, and whose free-energy density grows steeply away from its minima.

2. Micromagnetics

2.1. The free energy of micromagnetics

The most widely accepted continuum model of the behavior of magnetoelastic solids is a version of micromagnetics. Although the name and the systematic development of a conceptual framework are due to Brown (1963), some of the main ideas were already presented by Landau and Lifschitz (1935). The starting point for our theory is a small strain version of this canonical variational model, that Brown calls the conventional theory of magnetostriction (Brown, 1966), see also DeSimone (1994).

We consider a reference configuration Ω, i.e., a smooth, regular region of $\mathbb{R}^3$. The theory is appropriate for single crystals, and Ω represents a region occupied by the undistorted crystalline solid. We denote by $\boldsymbol{m}(\boldsymbol{x})$ the *magnetization* at a point $\boldsymbol{x} \in \Omega$. At a fixed temperature below the Curie point, the magnitude of the vector field $\boldsymbol{m}$ on Ω is a positive material constant

$$|\boldsymbol{m}(\boldsymbol{x})| \equiv m_{\mathrm{s}}, \quad \boldsymbol{x} \in \Omega \tag{2.1}$$

called saturation magnetization. We assume that $\boldsymbol{m} \in L^2(\Omega, m_{\mathrm{s}}S^2)$, where $m_{\mathrm{s}}S^2$ denotes the three-dimensional sphere of radius m_{s}, and we extend $\boldsymbol{m}$ to $\mathbb{R}^3$ by setting $\boldsymbol{m} = 0$

[1] Part of the results reported herein have been announced in DeSimone and James (1997).

outside Ω. The resulting space of admissible magnetizations will be denoted by $\mathscr{M}$. Furthermore, we denote by $\boldsymbol{y}:\Omega\to\mathbb{R}^3$ the *deformation* of the body so that the displacement at each point $\boldsymbol{x}\in\Omega$ is $\boldsymbol{u}(\boldsymbol{x})=\boldsymbol{y}(\boldsymbol{x})-\boldsymbol{x}$, and we denote the infinitesimal strain corresponding to $\boldsymbol{y}$ by

$$\begin{aligned}\boldsymbol{E}[\boldsymbol{y}](\boldsymbol{x}) &= \tfrac{1}{2}(\nabla\boldsymbol{y}(\boldsymbol{x})+(\nabla\boldsymbol{y}(\boldsymbol{x}))^{\mathrm{T}})-\boldsymbol{I},\\ &= \tfrac{1}{2}(\nabla\boldsymbol{u}(\boldsymbol{x})+(\nabla\boldsymbol{u}(\boldsymbol{x}))^{\mathrm{T}})\end{aligned} \tag{2.2}$$

with $\boldsymbol{I}$ the identity matrix and the superscript T denoting the transpose. We assume that $\boldsymbol{y}\in H^1(\Omega,\mathbb{R}^3)$. Associated with each magnetization vector, there exists a preferred local distortion of the crystalline lattice. This correspondence is described by the even function

$$\boldsymbol{m}\mapsto\boldsymbol{E}_0(\boldsymbol{m})\in M^{3\times3}_{\mathrm{sym}}, \tag{2.3}$$

where $M^{3\times3}_{\mathrm{sym}}$ is the set of symmetric 3×3 matrices. We refer to $\boldsymbol{E}_0(\boldsymbol{m})$ as the stress-free strain corresponding to the magnetization $\boldsymbol{m}$.

In a crystalline solid, there exist preferred directions of magnetization, which are modeled through an even, non-negative *anisotropy energy density* $\varphi: m_{\mathrm{s}}S^2\to[0,+\infty)$. The zeroes of φ define the easy axes, i.e., the directions along which the material is magnetized most easily. If $\bar{\boldsymbol{m}}$ is on an easy axis, and $\bar{\boldsymbol{E}}=\boldsymbol{E}_0(\bar{\boldsymbol{m}})$ is the corresponding stress-free strain, then the pair $(\bar{\boldsymbol{E}},\bar{\boldsymbol{m}})$ minimizes the (total) *anistropy energy density* Φ: $M^{3\times3}_{\mathrm{sym}}\times m_{\mathrm{s}}S^2\to[0,+\infty)$, defined by

$$\Phi(\boldsymbol{E},\boldsymbol{m})=\varphi(\boldsymbol{m})+\tfrac{1}{2}(\boldsymbol{E}-\boldsymbol{E}_0(\boldsymbol{m}))\cdot\mathbb{C}(\boldsymbol{E}-\boldsymbol{E}_0(\boldsymbol{m})). \tag{2.4}$$

Here, $\mathbb{C}$ is the (positive-definite) fourth-order tensor of the elastic moduli (note that the classical stored energy density of linear elasticity is obtained from Eq. (2.4) if φ and $\boldsymbol{E}_0$ vanish identically). The energy density Φ is invariant under material symmetry transformations

$$\Phi(\boldsymbol{QEQ}^{\mathrm{T}},\boldsymbol{Qm})=\Phi(\boldsymbol{E},\boldsymbol{m})\quad\forall Q\in P, \tag{2.5}$$

where $P\subset O(3)$ is the finite point group of the undistorted crystalline lattice associated to Ω. It follows then from Eq. (2.5) that φ, $\mathbb{C}$ and $\boldsymbol{E}_0$ are invariant under material symmetry transformations

$$\begin{aligned}&\boldsymbol{QEQ}^{\mathrm{T}}\cdot\mathbb{C}\boldsymbol{QEQ}^{\mathrm{T}}=\boldsymbol{E}\cdot\mathbb{C}\boldsymbol{E},\quad \boldsymbol{E}_0(\boldsymbol{Qm})=\boldsymbol{QE}_0(\boldsymbol{m})\boldsymbol{Q}^{\mathrm{T}},\\ &\quad\text{and } \varphi(\boldsymbol{Qm})=\varphi(\boldsymbol{m})\quad\forall\boldsymbol{Q}\in P.\end{aligned} \tag{2.6}$$

Moreover, if $(\bar{\boldsymbol{E}},\bar{\boldsymbol{m}})$ is a zero of Φ, so is $(\boldsymbol{Q}\bar{\boldsymbol{E}}\boldsymbol{Q}^{\mathrm{T}},\boldsymbol{Q}\bar{\boldsymbol{m}})$ for each $\boldsymbol{Q}\in P$. We assume that all minimizers of Φ are generated from a single one by symmetry transformations. Thus, the zero-level set of the energy density Φ, which we denote by $\mathbb{K}$, has the structure

$$\mathbb{K}=\bigcup_{i=1}^{n}(\boldsymbol{E}_i,\pm\boldsymbol{m}_i), \tag{2.7}$$

and for each $j=1,\dots,n$, there exists a symmetry transformation $\boldsymbol{Q}\in P$ such that $(\boldsymbol{E}_j,\boldsymbol{m}_j)=(\boldsymbol{QE}_1\boldsymbol{Q}^{\mathrm{T}},\boldsymbol{Qm}_1)$. Each $(\boldsymbol{E},\boldsymbol{m})$ in $\mathbb{K}$ is called an *energy well*, so altogether there are $N=2n$ energy wells.

Every magnetized body generates a magnetic field permeating the whole ambient space. For a given magnetization $\boldsymbol{m} \in \mathscr{M}$, the induced field is the unique vector field $\boldsymbol{h}$ solving Maxwell's equations of magnetostatics

$$\left.\begin{aligned} &\operatorname{curl} \boldsymbol{h} = 0 \\ &\operatorname{div}(\boldsymbol{h} + 4\pi \boldsymbol{m}) = 0 \end{aligned}\right. \quad \text{in } \mathbb{R}^3 \tag{2.8}$$

and which is square integrable, i.e., $\boldsymbol{h} \in L^2(\mathbb{R}^3, \mathbb{R}^3)$. We denote the unique solution of Eq. (2.8) corresponding to the given $\boldsymbol{m}$ with either of the following notations:

$$\boldsymbol{h}_{\boldsymbol{m}} = -\nabla \zeta_{\boldsymbol{m}}, \tag{2.9}$$

where the equality is justified by the fact that $\boldsymbol{h}_{\boldsymbol{m}}$ is curl-free on $\mathbb{R}^3$. Associated with the induced magnetic field $\boldsymbol{h}_{\boldsymbol{m}}$ there is a non-local energy term, namely, the *magnetostatic energy*

$$\frac{1}{8\pi} \int_{\mathbb{R}^3} |\boldsymbol{h}_{\boldsymbol{m}}(\boldsymbol{x})|^2 \, \mathrm{d}\boldsymbol{x} = -\frac{1}{2} \int_{\Omega} \boldsymbol{h}_{\boldsymbol{m}}(\boldsymbol{x}) \cdot \boldsymbol{m}(\boldsymbol{x}) \, \mathrm{d}\boldsymbol{x} \tag{2.10}$$

(use of Eq. (2.8) justifies the equality). From Eq. (2.8) $\operatorname{div} \boldsymbol{m} = 0$ on $\mathbb{R}^3$ implies that $\boldsymbol{h}_{\boldsymbol{m}} = 0$; thus, divergence-free magnetizations generate no magnetostatic energy. It can easily be shown, based on Eq. (2.8), that the average magnetization is small if the magnetostatic energy is small, so divergence-free magnetizations are also associated with demagnetized states.

We assume also the presence of a constant applied magnetic field $\boldsymbol{h}$, which contributes an *applied field energy* $-\int_{\Omega} \boldsymbol{h} \cdot \boldsymbol{m}(\boldsymbol{x}) \, \mathrm{d}\boldsymbol{x}$. A large applied field can induce an energy minimizing uniform magnetization on Ω despite the demagnetizing influence of the magnetostatic energy. We also envisage a mechanical counterpart to this last energy term, a *loading device energy* given by $-\int_{\Omega} \boldsymbol{S} \cdot \boldsymbol{E}[\boldsymbol{y}](\boldsymbol{x}) \, \mathrm{d}\boldsymbol{x}$, generated by a constant 3×3 matrix $\boldsymbol{S}$. This term is the energy associated to an applied surface stress $\boldsymbol{S}\boldsymbol{n}(\boldsymbol{x})$. Since $\boldsymbol{S}$ is constant (in particular, independent of $\boldsymbol{y}$), this contribution to the energy describes the energy of a dead loading device.

The discussion above should motivate the following form for the free-energy functional, whose minimizers describe the macroscopic behavior of a magnetoelastic body Ω subjected to the applied magnetic field $\boldsymbol{h}$ and to the applied surface tractions $\boldsymbol{S}$:

$$\begin{aligned} \mathscr{E}(\boldsymbol{E}[\boldsymbol{y}], \boldsymbol{m}) = & \int_{\Omega} \Phi(\boldsymbol{E}[\boldsymbol{y}](\boldsymbol{x}), \boldsymbol{m}(\boldsymbol{x})) \, \mathrm{d}\boldsymbol{x} \\ & - \int_{\Omega} (\boldsymbol{S} \cdot \boldsymbol{E}[\boldsymbol{y}](\boldsymbol{x}) + \boldsymbol{h} \cdot \boldsymbol{m}(\boldsymbol{x})) \, \mathrm{d}\boldsymbol{x} + \frac{1}{8\pi} \int_{\mathbb{R}^3} |\nabla \zeta_{\boldsymbol{m}}(\boldsymbol{x})|^2 \, \mathrm{d}\boldsymbol{x}. \end{aligned} \tag{2.11}$$

The natural space for studying low-energy strains and magnetizations is

$$\mathscr{A} := \{(\boldsymbol{E}, \boldsymbol{m}) \colon \boldsymbol{E} = \boldsymbol{E}[\boldsymbol{y}] \text{ for some } \boldsymbol{y} \in H^1(\Omega, \mathbb{R}^3) \text{ and } \boldsymbol{m} \in \mathscr{M}\}. \tag{2.12}$$

Expression (2.11) is appropriate for large bodies. That is, it is missing the exchange term and this makes it unsuitable to study questions such as the geometry or the length scale of the domains. However, as explained rigorously in DeSimone (1993), there are many properties of interest, like local average strain, local average magnetization, and all of the information used in standard magnetomechanical measurements such as magnetization curves, strain vs. field, measurements of anisotropy and of magnetostriction constants, etc., that is obtainable by minimizing Eq. (2.11).

2.2. Energy wells, pairwise compatibility and crystalline symmetry

The set $\mathbb{K}$ of the energy wells of a crystalline solid enjoys symmetry properties which reflect the symmetries of the underlying atomic lattice. Of particular relevance to our analysis is the following one.

Definition 2.1. The set $\mathbb{K} = \bigcup_{i=1}^{N} \{\boldsymbol{E_i}, \boldsymbol{m_i}\}$ consists of N *pairwise compatible magnetoelastic wells* if there exist unit vectors $\boldsymbol{n}_{jk}$, and vectors $\boldsymbol{a}_{jk}$, $j,k = 1,\dots,N$ such that

$$\boldsymbol{E}_j - \boldsymbol{E}_k = \tfrac{1}{2}(\boldsymbol{a}_{jk} \otimes \boldsymbol{n}_{jk} + \boldsymbol{n}_{jk} \otimes \boldsymbol{a}_{jk}), \tag{2.13}$$

$$(\boldsymbol{m}_j - \boldsymbol{m}_k) \cdot \boldsymbol{n}_{jk} = 0 \tag{2.14}$$

for all $j,k = 1,\dots,N$.

To explain the physical motivation behind Definition 2.1, let's examine the case $N = 2$. Eq. (2.13) is the familiar Hadamard jump condition, which is necessary and sufficient for the existence of a nontrivial (i.e., nonaffine) continuous deformation $\boldsymbol{y}$ such that $\boldsymbol{E}[\boldsymbol{y}] \in \{\boldsymbol{E}_1, \boldsymbol{E}_2\}$. In the case that $\boldsymbol{E}_1 \neq \boldsymbol{E}_2$, $\boldsymbol{n}_{12}$ and $\boldsymbol{a}_{12}$ are the normals to the surfaces of discontinuity of the strain. Then, (2.14) is the condition that the interfaces with normal $\boldsymbol{n}_{12}$ serve as pole-free surfaces of discontinuity of the magnetization.[2]

A natural question needs to be addressed: Do 'real' materials give rise to pairwise compatible magnetoelastic wells? Surprisingly, this turns out to be the rule, rather than the exception, as we argue in the remainder of this section. The reason behind this is that the wells are not arbitrary, but they satisfy special relations due to material symmetry.

In the case of crystalline solids, the number of wells is even ($N = 2n$), the set $\mathbb{K}$ is of the form

$$\mathbb{K} = \bigcup_{i=1}^{n} \{(\boldsymbol{E}_i, \boldsymbol{m}_i), (\boldsymbol{E}_i, -\boldsymbol{m}_i)\}$$

and the variants comprising $\mathbb{K}$ are related to one another by symmetry transformations

$$(\boldsymbol{E}_j, \pm \boldsymbol{m}_j) = (\boldsymbol{Q}\boldsymbol{E}_k\boldsymbol{Q}^{\mathrm{T}}, \pm \boldsymbol{Q}\boldsymbol{m}_k) \tag{2.15}$$

for some $\boldsymbol{Q} \in SO(3)$ in the point group P of the undistorted crystalline lattice. In the special case in which $\boldsymbol{Q}$ is also in the point group of the lattice deformed according to $\boldsymbol{E}_k$, formula (2.15) gives $\boldsymbol{E}_j = \boldsymbol{E}_k$. In these circumstances, satisfying magnetoleastic compatibility between $(\boldsymbol{E}_k, \boldsymbol{m}_k)$ and $(\boldsymbol{E}_k, \boldsymbol{m}_j)$ reduces to finding an interface with normal

[2] While (2.13) is truly a compatibility condition on $\boldsymbol{E}_1$, $\boldsymbol{E}_2$, (2.14) can be violated at a finite energy cost (precisely: at the expense of some excess magnetostatic energy) by an admissible magnetization with values $\boldsymbol{m}_1$, $\boldsymbol{m}_2$.

$\boldsymbol{n}$ for which $\boldsymbol{m}_j$ and $\boldsymbol{m}_k$ are magnetically compatible: $(\boldsymbol{m}_j - \boldsymbol{m}_k) \cdot \boldsymbol{n} = 0$. Since this condition can be easily satisfied, we will focus, in the rest of our discussion, on the case $\boldsymbol{E}_j \neq \boldsymbol{E}_k$.

Now, as it is well known from the literature on diffusionless solid-to-solid phase transformations, see e.g. Ball and James (1992) and Bhattacharya (1993), the kinematic compatibility condition between the strain tensors $\boldsymbol{E}_j$ and $\boldsymbol{E}_k$ is automatically satisfied if there exists a 180° rotation $\boldsymbol{Q}$ such that

$$\boldsymbol{Q}\boldsymbol{E}_k\boldsymbol{Q}^{\mathrm{T}} = \boldsymbol{E}_j, \quad \boldsymbol{Q} = -\boldsymbol{I} + 2\boldsymbol{b} \otimes \boldsymbol{b} \tag{2.16}$$

(here the unit vector $\boldsymbol{b}$ identifies the axis of the rotation $\boldsymbol{Q}$). Indeed, granted (2.16), and letting $\boldsymbol{a} = 4[(\boldsymbol{E}_i \cdot \boldsymbol{b} \otimes \boldsymbol{b})\boldsymbol{b} - \boldsymbol{E}_i\boldsymbol{b}]$ we have

$$\boldsymbol{E}_j - \boldsymbol{E}_k = \tfrac{1}{2}(\boldsymbol{a} \otimes \boldsymbol{b} + \boldsymbol{b} \otimes \boldsymbol{a}).$$

We can thus form planar interfaces separating regions of the body deformed according to $\boldsymbol{E}_k$ and $\boldsymbol{E}_j$ (i.e., twins) either with normal $\boldsymbol{n}_{\mathrm{I}} = \boldsymbol{b}$, or with normal $\boldsymbol{n}_{\mathrm{II}} = \boldsymbol{a}$. In the former case $\boldsymbol{Q}\boldsymbol{n}_{\mathrm{I}} = \boldsymbol{n}_{\mathrm{I}}$, and the twin is of type I, while in the latter $\boldsymbol{Q}\boldsymbol{n}_{\mathrm{II}} = -\boldsymbol{n}_{\mathrm{II}}$ and the twin is of type II. Under the addtional assumptions that $\boldsymbol{Q}$ is a symmetry transformation, i.e., it satisfies Eq. (2.15), and that there exists a unique easy magnetic direction associated with each $\boldsymbol{E}_i$, so that

$$\boldsymbol{m}_j = \pm\, \boldsymbol{Q}\boldsymbol{m}_k \tag{2.17}$$

the magnetic compatibility between the variants k and j becomes a consequence of their elastic compatibility. Indeed, if $\boldsymbol{m}_j = \boldsymbol{Q}\boldsymbol{m}_k$, then

$$(\boldsymbol{m}_j - \boldsymbol{m}_k) \cdot \boldsymbol{n}_{\mathrm{I}} = (\boldsymbol{m}_k - \boldsymbol{m}_k) \cdot \boldsymbol{Q}\boldsymbol{n}_{\mathrm{I}} = 0$$

and we can achieve magnetoelastic compatibility by taking $\boldsymbol{a}_{jk} = \boldsymbol{a}$, $\boldsymbol{n}_{jk} = \boldsymbol{n}_{\mathrm{I}} = \boldsymbol{b}$. If $\boldsymbol{m}_j = -\boldsymbol{Q}\boldsymbol{m}_k$, then

$$(\boldsymbol{m}_j - \boldsymbol{m}_k) \cdot \boldsymbol{n}_{\mathrm{II}} = \boldsymbol{m}_k \cdot \boldsymbol{n}_{\mathrm{II}} - \boldsymbol{m}_k \cdot \boldsymbol{n}_{\mathrm{II}} = 0$$

and we can take $\boldsymbol{a}_{jk} = \boldsymbol{b}$, $\boldsymbol{n}_{jk} = \boldsymbol{n}_{\mathrm{II}} = \boldsymbol{a}$.

Remark. The proof given above that kinematic compatibility implies magnetic compatibility rests on the two assumptions

1. There exists a symmetry transformation $\boldsymbol{Q} \in P$ satisfying Eq. (2.16).
2. There exists a unique magnetic direction associated with each $\boldsymbol{E}_i$

so that Eqs. (2.16) and (2.17) hold simultaneously. Although the validity of these two assumptions is not universal, they prove sufficient to handle most of the cases of practical interest. It is even possible to extend the argument to the case of large deformations (at the expense of some additional assumptions, see, James and Hane, 2000; James and Kinderlehrer, 1993; James and Wuttig, 1998).

3. A constrained theory for large magnetoelastic moduli

3.1. Magnetoelastic moduli and constraints on Young measures

We aim for a theory which is valid for small applied fields and loads relative to the appropriate magnetoelastic moduli. To make ideas concrete, let us adopt the particular form of the magnetocrystalline anisotropy energy given by

$$\varphi(\boldsymbol{m}) = K(\alpha_1^2\alpha_2^2 + \alpha_1^2\alpha_3^2 + \alpha_2^2\alpha_3^2 - \tfrac{1}{3}),$$
$$K < 0, \quad \boldsymbol{m} = m_s(\alpha_i \boldsymbol{e}^i). \tag{3.1}$$

Here $\{\boldsymbol{e}^i\}$ is an orthonormal basis and this expression is appropriate for a cubic crystal with easy axes along [1 1 1] directions, such as Terfenol-D. The easy axes and corresponding preferred strains in this case are $(\boldsymbol{E}_1, \pm\boldsymbol{m}_1), \ldots, (\boldsymbol{E}_4, \pm\boldsymbol{m}_4)$ where

$$\boldsymbol{m}_1 = \frac{m_s}{\sqrt{3}}(1,\, 1,\, 1), \qquad \boldsymbol{E}_1 = \boldsymbol{E}_0(\boldsymbol{m}_1),$$
$$\boldsymbol{m}_2 = \frac{m_s}{\sqrt{3}}(-1,\, 1,\, 1), \quad \boldsymbol{E}_2 = \boldsymbol{E}_0(\boldsymbol{m}_2),$$
$$\boldsymbol{m}_3 = \frac{m_s}{\sqrt{3}}(1,\, -1,\, 1), \quad \boldsymbol{E}_3 = \boldsymbol{E}_0(\boldsymbol{m}_3),$$
$$\boldsymbol{m}_4 = \frac{m_s}{\sqrt{3}}(1,\, 1,\, -1), \quad \boldsymbol{E}_4 = \boldsymbol{E}_0(\boldsymbol{m}_4), \tag{3.2}$$

We emphasize that the particular forms (3.1) and (3.2) are not essential for our subsequent results: any finite number of energy wells would be acceptable. We wish to assume that the applied stress and field are much smaller than the corresponding elastic and magnetocrystalline moduli. However, the total energy also contains other dimensional quantities. In typical applications we expect that the energy of the applied stress and applied field will neither dominate, nor be dominated by, the magnetostatic energy. To ensure that this balance is maintained, it is convenient to keep $\boldsymbol{h}$ and $\boldsymbol{S}$ fixed and let the moduli $|K|, |\mathbb{C}\,| \to \infty$. To understand this limit in terms of dimensionless numbers, we first note that the magnetostatic equation (2.10) is nondimensionalized by dividing it by $\sqrt{2\pi}m_s$. (The presence of the factor $\sqrt{2\pi}$ is the usual convention). This scales the magnetostatic potential by the same factor, which in turn scales the magnetostatic energy by the factor $2\pi m_s^2$. Hence, a convenient nondimensionalization is to divide the whole energy by $2\pi m_s^2$. This yields the nondimensional moduli $K/2\pi m_s^2$ and $\mathbb{C}/2\pi m_s^2$. So, the regime of interest here is governed by

$$\frac{|K|}{2\pi m_s^2} \to \infty, \quad \frac{|\mathbb{C}\,|}{2\pi m_s^2} \to \infty, \tag{3.3}$$

$$\frac{|\boldsymbol{S}|}{2\pi m_s^2} \leqslant 0(1), \quad \frac{m_s|\boldsymbol{h}|}{2\pi m_s^2} \leqslant 0(1). \tag{3.4}$$

For simplicity we introduce a single dimensionless parameter $k = 1, 2, \ldots$, and let $K = K_k = kK_1$ and $\mathbb{C} = \mathbb{C}_k = k\mathbb{C}_1$ with $K_1 < 0$ and $\mathbb{C}_1$ positive-definite. Note that the set of the energy wells (3.2), denoted by $\mathbb{K}$, is invarariant with this rescaling of the magnetoelastic moduli.

Also, we let φ_k be given by Eq. (3.1) with K replaced by K_k and we denote the total energy (2.11) with $K = K_k$ and $\mathbb{C} = \mathbb{C}_k$ by $\mathscr{E}_k$.

Let us now move to the study of the energetics of strain and magnetization pairs in the space $\mathscr{A}$ defined in Eq. (2.12). Generally, there is no exact minimizer of $\mathscr{E}_k$ (for k fixed) in $\mathscr{A}$. This is a byproduct of our having omitted strain-gradient and exchange energies, and as described above, is appropriate for large bodies. Hence, we shall study the asymptotic behavior of 'low energy strain-magnetization pairs': these are strain-magnetization pairs $(\boldsymbol{E}, \boldsymbol{m}) \in \mathscr{A}$ whose energy differs from the infimum of $\mathscr{E}_k$ by some specific tolerance

$$\mathscr{E}_k(\boldsymbol{E}, \boldsymbol{m}) \leqslant \inf_{\mathscr{A}} \mathscr{E}_k + \frac{1}{k}. \tag{3.5}$$

Then, studying the behavior of the infimum of $\mathscr{E}_k$ as k tends to infinity leads to studying the asymptotic behavior of sequences of low-energy-strain-magnetization pairs $(\boldsymbol{E}^{(k)}, \boldsymbol{m}^{(k)}) \in \mathscr{A}$, $k = 1, 2, \ldots$. The main technical tools to describe this asymptotic behavior are weak convergence and Young measures. Their basic properties are summarized in Appendix A.2. To keep the paper self-contained, Appendix A.2 is written so as to be approachable to the nonspecialist.

Intuitively, it is expected that as the magnetoelastic moduli get large the corresponding low-energy pairs $(\boldsymbol{E}^{(k)}(\boldsymbol{x}), \boldsymbol{m}^{(k)}(\boldsymbol{x}))$, will lie near the energy wells $\mathbb{K}$ for all $\boldsymbol{x} \in \Omega$. However, because the anisotropy energy in Eq. (2.11) is an integral over Ω, then if $(\boldsymbol{E}^{(k)}(\boldsymbol{x}), \boldsymbol{m}^{(k)}(\boldsymbol{x}))$ depart from the wells (but remain bounded) on a subset of Ω of sufficiently small volume, say, a volume of $1/k^2$, then such a departure will cost negligible energy, since the moduli K_k and $\mathbb{C}_k$ grow like k. Such regions of departure represent thin layers between magnetoelastic domains. As explained further below, see Section 3.2, it is extremely important to allow such transition layers to be present.

Theorem 3.1. *Let $(\boldsymbol{E}^{(k)}, \boldsymbol{m}^{(k)}) \in \mathscr{A}$ be a sequence of low-energy strain-magnetization pairs in the sense that*

$$\mathscr{E}_k(\boldsymbol{E}^{(k)}, \boldsymbol{m}^{(k)}) \leqslant \inf_{\mathscr{A}} \mathscr{E}_k + \frac{1}{k}. \tag{3.6}$$

After passing to a suitable subsequence (*not relabeled*), *we may associate a Young measure $\nu_{\boldsymbol{x}}$ to $(\boldsymbol{E}^{(k)}, \boldsymbol{m}^{(k)})$. This measure is supported on the energy wells*

$$\operatorname{supp} \nu_{\boldsymbol{x}} \subset \mathbb{K}, \in \Omega \tag{3.7}$$

almost everywhere in Ω, see Eq. (A.4), *and the sequence minimizes the limiting applied and magnetostatic energies alone*

$$\begin{aligned} &\lim_{k\to\infty} \int_\Omega -\boldsymbol{h} \cdot \boldsymbol{m}^{(k)} - \boldsymbol{S} \cdot \boldsymbol{E}^{(k)} \, \mathrm{d}\boldsymbol{x} + \frac{1}{8\pi} \int_{\mathbb{R}^3} |\nabla \zeta_{\boldsymbol{m}^{(k)}}|^2 \, \mathrm{d}\boldsymbol{x} \\ &\quad \leqslant \lim_{k\to\infty} \int_\Omega -\boldsymbol{h} \cdot \hat{\boldsymbol{m}}^{(k)} - \boldsymbol{S} \cdot \hat{\boldsymbol{E}}^{(k)} \, \mathrm{d}\boldsymbol{x} + \frac{1}{8\pi} \int_{\mathbb{R}^3} |\nabla \zeta_{\hat{\boldsymbol{m}}^{(k)}}|^2 \, \mathrm{d}\boldsymbol{x} \end{aligned} \tag{3.8}$$

for all sequences $(\hat{\boldsymbol{m}}^{(k)}, \hat{\boldsymbol{E}}^{(k)})$ *in* $\mathscr{A}$ *having Young measures supported on* $\mathbb{K}$. *Here, it is assumed that further subsequences are taken, if necessary, so that the two limits in Eq.* (3.8) *exist.*

Proof. Since the magnetostatic energy is bounded, we can assume without loss of generality that $\lim_{k\to\infty} \int_{\mathbb{R}^3} |\nabla\zeta_{\boldsymbol{m}^{(k)}}|^2 \, \mathrm{d}\boldsymbol{x}$ exists. Denote the total anisotropy energy density by $\Phi_k(\boldsymbol{E}, \boldsymbol{m}) = k\Phi_1(\boldsymbol{E}, \boldsymbol{m})$. Let $(\boldsymbol{E}_0, \boldsymbol{m}_0)$ be any constant strain-magnetization pair on $\mathbb{K}$, and compare the total energy of $(\boldsymbol{E}^{(k)}, \boldsymbol{m}^{(k)})$ with that of the uniform state $(\boldsymbol{E}(\boldsymbol{x}), \boldsymbol{m}(\boldsymbol{x})) \equiv (\boldsymbol{E}_0, \boldsymbol{m}_0)$:

$$\begin{aligned}\int_\Omega &(k\Phi_1(\boldsymbol{E}^{(k)}(\boldsymbol{x}), \boldsymbol{m}^{(k)}(\boldsymbol{x})) - \boldsymbol{h}\cdot\boldsymbol{m}^{(k)}(\boldsymbol{x}) \\ &\quad - \boldsymbol{S}\cdot\boldsymbol{E}^{(k)}(\boldsymbol{x}))\,\mathrm{d}\boldsymbol{x} + \frac{1}{8\pi}\int_{\mathbb{R}^3} |\nabla\zeta_{\boldsymbol{m}^{(k)}}(\boldsymbol{x})|^2\,\mathrm{d}\boldsymbol{x} \\ &\leqslant -\int (\boldsymbol{h}\cdot\boldsymbol{m}_0 + \boldsymbol{S}\cdot\boldsymbol{E}_0)\,\mathrm{d}\boldsymbol{x} + \frac{1}{8\pi}\int_{\mathbb{R}^3} |\nabla\zeta_{\boldsymbol{m}_0}|^2\,\mathrm{d}\boldsymbol{x} + \frac{1}{k}. \end{aligned} \tag{3.9}$$

Thus

$$\int_\Omega \Phi_1(\boldsymbol{E}^{(k)}(\boldsymbol{x}), \boldsymbol{m}^{(k)}(\boldsymbol{x}))\,\mathrm{d}\boldsymbol{x} \to 0 \text{ as } k\to\infty \tag{3.10}$$

for a suitable subsequence (not relabelled), with Young measure $\nu_{\boldsymbol{x}}$. From (A.4), supp $\nu_{\boldsymbol{x}} \subset \mathbb{K}$. Since Eq. (3.10) can be made to go to zero with arbitrary rate by choosing rarer and rarer subsequences, let us choose a subsequence $\{\tilde{\boldsymbol{E}}^{(k)}, \tilde{\boldsymbol{m}}^{(k)}\} \subset \{\boldsymbol{E}^{(k)}, \boldsymbol{m}^{(k)}\}$ with the property

$$\int_\Omega k\Phi_1(\tilde{\boldsymbol{E}}^{(k)}, \tilde{\boldsymbol{m}}^{(k)})\,\mathrm{d}\boldsymbol{x} \to 0, \quad k = 1, 2, \ldots \tag{3.11}$$

Now compare the energy of the original sequence to the energy of $(\tilde{\boldsymbol{E}}^{(k)}, \tilde{\boldsymbol{m}}^{(k)})$

$$\begin{aligned}\int_\Omega &(k\Phi_1(\boldsymbol{E}^{(k)}(\boldsymbol{x}), \boldsymbol{m}^{(k)}(\boldsymbol{x})) - \boldsymbol{h}\cdot\boldsymbol{m}^{(k)}(\boldsymbol{x}) - \boldsymbol{S}\cdot\boldsymbol{E}^{(k)}(\boldsymbol{x}))\,\mathrm{d}\boldsymbol{x} + \frac{1}{8\pi}\int_{\mathbb{R}^3} |\nabla\zeta_{\boldsymbol{m}^{(k)}}|^2\,\mathrm{d}\boldsymbol{x} \\ &\leqslant \int_\Omega (k\Phi_1(\tilde{\boldsymbol{E}}^{(k)}(\boldsymbol{x}), \tilde{\boldsymbol{m}}^{(k)}(\boldsymbol{x})) - \boldsymbol{h}\cdot\tilde{\boldsymbol{m}}^{(k)}(\boldsymbol{x}) \\ &\quad - \boldsymbol{S}\cdot\tilde{\boldsymbol{E}}^{(k)}(\boldsymbol{x}))\,\mathrm{d}\boldsymbol{x} + \frac{1}{8\pi}\int |\nabla\zeta_{\tilde{\boldsymbol{m}}^{(k)}}|^2\,\mathrm{d}\boldsymbol{x} + \frac{1}{k}. \end{aligned} \tag{3.12}$$

Passing to the limit in Eq. (3.12) and using the fact that $(\tilde{\boldsymbol{E}}^{(k)}, \tilde{\boldsymbol{m}}^{(k)})$ is a subsequence of $(\boldsymbol{E}^{(k)}, \boldsymbol{m}^{(k)})$, we get that

$$\int_\Omega k\Phi_1(\boldsymbol{E}^{(k)}(\boldsymbol{x}), \boldsymbol{m}^{(k)}(\boldsymbol{x}))\,\mathrm{d}\boldsymbol{x} \to 0. \tag{3.13}$$

This gives the left-hand side of Eq. (3.10) as the limiting energy of $(\boldsymbol{E}^{(k)}, \boldsymbol{m}^{(k)})$. Now consider a test sequence $(\hat{\boldsymbol{E}}^{(k)}, \hat{\boldsymbol{m}}^{(k)}) \rightharpoonup (\hat{\boldsymbol{E}}, \hat{\boldsymbol{m}})$ in L^2 whose Young measure has support on the wells. Using a similar strategy as in Eqs. (3.10)–(3.13), extract a sufficiently rare subsequence with the property that its anisotropy energy converges to zero. Comparing the energy of this sequence with the energy of $(\boldsymbol{E}^{(k)}, \boldsymbol{m}^{(k)})$ we get Eq. (3.8). $\square$

The theorem above shows that, in the material parameter regime described by Eqs. (3.3), (3.4) one has a variational principal for sequences

$$\begin{aligned}\lim_{k\to\infty}(\inf_{\mathscr{A}}\mathscr{E}_k) = &\inf_{\mathscr{S}}\left(\lim_{k\to\infty}\mathscr{E}_k(\boldsymbol{E}[\boldsymbol{y}^{(k)}], \boldsymbol{m}^{(k)})\right)\\ &= \inf_{\mathscr{S}}\left(\lim_{k\to\infty}\left(-\int_\Omega \boldsymbol{h}\cdot\boldsymbol{m}^{(k)} + \boldsymbol{S}\cdot\boldsymbol{E}[\boldsymbol{y}^{(k)}]\,\mathrm{d}\boldsymbol{x}\right.\right.\\ &\qquad\left.\left.+\frac{1}{8\pi}\int_{\mathbb{R}^3}|\nabla\zeta_{\boldsymbol{m}^{(k)}}|^2\,\mathrm{d}\boldsymbol{x}\right)\right), \qquad (3.14)\end{aligned}$$

where

$$\mathscr{S} = \{\text{sequences } (\boldsymbol{E}^{(k)}, \boldsymbol{m}^{(k)}) \quad \text{in } \mathscr{A} \text{ such that (3.7) holds}\} \qquad (3.15)$$

is the set of admissible sequences generating Young measures supported on $\mathbb{K}$. In this way, we have replaced the problem of minimizing Eq. (2.11) with Eq. (3.14). In order to make this new minimization problem more explicit, we would like now to pass to the limit in Eq. (3.14). Before tackling the general case, we will build up some intuition on the asymptotic properties of infinitely refining sequences in a simple example, which involves only two energy wells.

3.2. An example: two energy wells and simple layering

Referring to Fig. 2, let $\boldsymbol{E}_a$, $\boldsymbol{E}_b \in M^{3\times3}_{\text{sym}}$ be two strains satisfying

$$\boldsymbol{E}_b - \boldsymbol{E}_a = \tfrac{1}{2}(\boldsymbol{a}\otimes\boldsymbol{n} + \boldsymbol{n}\otimes\boldsymbol{a}) \qquad (3.16)$$

for some vector $\boldsymbol{a}$ and unit vector $\boldsymbol{n}$. For $\boldsymbol{x}\in\Omega$, and $k = 1, 2, \ldots$, let

$$\boldsymbol{y}^{(k)}(\boldsymbol{x}) = \boldsymbol{c} + \boldsymbol{F}_b\boldsymbol{x} - \frac{1}{k}\boldsymbol{a}\int_0^{k\boldsymbol{x}\cdot\boldsymbol{n}}\chi_\lambda(s)\,\mathrm{d}s, \qquad (3.17)$$

$$\boldsymbol{m}^{(k)}(\boldsymbol{x}) = \chi_\lambda(k\boldsymbol{x}\cdot\boldsymbol{n})\boldsymbol{m}_a + (1-\chi_\lambda(k\boldsymbol{x}\cdot\boldsymbol{n}))\boldsymbol{m}_b, \qquad (3.18)$$

where $\lambda\in[0,1]$, $\boldsymbol{F}_b = \boldsymbol{I} + \boldsymbol{E}_b + \boldsymbol{W}_b$, $\boldsymbol{W}_b = (1-\lambda)/2(\boldsymbol{a}\otimes\boldsymbol{n} - \boldsymbol{n}\otimes\boldsymbol{a})$, $\boldsymbol{m}_a$, $\boldsymbol{m}_b \in m_{\mathrm{s}}S^2$, χ_λ is the one-periodic function such that

$$\chi_\lambda(s) = \begin{cases} 1 & \text{if } s\in[0,\lambda],\\ 0 & \text{if } s\in[\lambda,1]\end{cases} \qquad (3.19)$$

and $\boldsymbol{c}\in\mathbb{R}^3$ is an arbitrary constant. Clearly $(\boldsymbol{E}[\boldsymbol{y}^{(k)}], \boldsymbol{m}^{(k)})\in\mathscr{A}$ for every k, and a short calculation shows that $(\boldsymbol{E}[\boldsymbol{y}^{(k)}](\boldsymbol{x}), \boldsymbol{m}^{(k)}(\boldsymbol{x})) = (\boldsymbol{E}_b, \boldsymbol{m}_b)$ on the 'layers' orthogonal to $\boldsymbol{n}$ and of width $(1-\lambda)/k$ where χ_λ takes the value zero. Moreover, setting $\boldsymbol{F}_a = \boldsymbol{F}_b - \boldsymbol{a}\otimes\boldsymbol{n}$, and $\boldsymbol{W}_a = -\lambda/2(\boldsymbol{a}\otimes\boldsymbol{n} - \boldsymbol{n}\otimes\boldsymbol{a})$, we have that $\boldsymbol{F}_a = \boldsymbol{I} + \boldsymbol{E}_a + \boldsymbol{W}_a$, and on the alternate layers where χ_λ is equal to one, $(\boldsymbol{E}[\boldsymbol{y}^{(k)}](\boldsymbol{x}), \boldsymbol{m}^{(k)}(\boldsymbol{x})) = (\boldsymbol{E}_a, \boldsymbol{m}_a)$. The deformation gradient

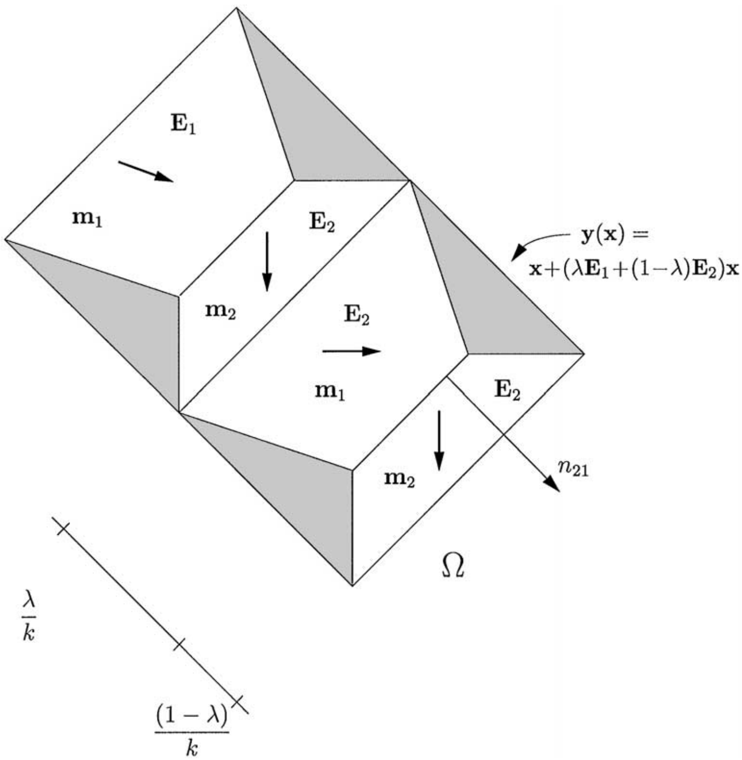

Fig. 2. A drawing of a simple laminate matching the boundary condition $\boldsymbol{y}^{(k)}(\boldsymbol{x}) = (\boldsymbol{I} + \boldsymbol{G})\boldsymbol{x}$ on $\partial\Omega$, with $\boldsymbol{G} = \lambda\boldsymbol{E}_1 + (1 - \lambda)\boldsymbol{E}_1$ and $\lambda \neq 0, 1$. As $k \to \infty$, the width of the boundary layer, shown in grey, tends to zero.

takes the values $\boldsymbol{F}_a$ and $\boldsymbol{F}_b$, and it may jump across the layer interfaces. However, $\boldsymbol{y}^{(k)}$ is continuous, and $\nabla\boldsymbol{y}^{(k)}$ satisfies the kinematic compatibility condition

$$\boldsymbol{F}_b - \boldsymbol{F}_a = \boldsymbol{a} \otimes \boldsymbol{n}$$

the large deformation version of Eq. (3.16). From this formula and Eq. (3.17) it follows that $\boldsymbol{y}^{(k)}$ converges uniformly to an affine function

$$\boldsymbol{y}^{(k)} \to \boldsymbol{c} + (\lambda\boldsymbol{F}_a + (1 - \lambda)\boldsymbol{F}_b)\boldsymbol{x}. \tag{3.20}$$

Our choice of the skew-symmetric matrices $\boldsymbol{W}_a, \boldsymbol{W}_b$ guarantees that

$$\lambda\boldsymbol{W}_a + (1 - \lambda)\boldsymbol{W}_b = 0 \tag{3.21}$$

i.e., the limiting average rigid body rotation accompanying $\boldsymbol{y}^{(k)}$ vanishes

$$\lim_{k\to\infty} \frac{1}{|\Omega|} \int_\Omega (\nabla\boldsymbol{y}^{(k)}(\boldsymbol{x}) - \nabla^T\boldsymbol{y}^{(k)}(\boldsymbol{x}))\,\mathrm{d}\boldsymbol{x} = 0.$$

Turning to the asymptotic features of the sequence of strain–deformation pairs associated with Eqs. (3.17)–(3.18), we have that $(\boldsymbol{E}[\boldsymbol{y}^{(k)}], \boldsymbol{m}^{(k)}) \rightharpoonup (\boldsymbol{E}^\infty, \boldsymbol{m}^\infty)$ in $L^2(\Omega)$, where

$$\boldsymbol{E}^{\infty} = \lambda \boldsymbol{E}_a + (1-\lambda)\boldsymbol{E}_b, \tag{3.22}$$

$$\boldsymbol{m}^{\infty} = \lambda \boldsymbol{m}_a + (1-\lambda)\boldsymbol{m}_b \tag{3.23}$$

and the sequence generates the $\boldsymbol{x}$-independent Young measure

$$\nu = \lambda \delta_{(\boldsymbol{E}_a,\boldsymbol{m}_a)} + (1-\lambda)\delta_{(\boldsymbol{E}_b,\boldsymbol{m}_b)}, \tag{3.24}$$

where $\delta_{\boldsymbol{A}}$ denotes a Dirac mass at $\boldsymbol{A}$. Note that Eq. (3.24) implies that $\operatorname{supp}\nu = \{(\boldsymbol{E}_a,\boldsymbol{m}_a),(\boldsymbol{E}_b,\boldsymbol{m}_b)\}$. Finally, we also note that, with Eqs. (3.21), (3.22), we can rewrite Eq. (3.20) as

$$\boldsymbol{y}^{(k)} \to \ \boldsymbol{c} + (\boldsymbol{I} + \boldsymbol{E}^{\infty})\boldsymbol{x} \quad \text{uniformly}. \tag{3.25}$$

The physical meaning of Eqs. (3.22)–(3.24) as macroscopically measurable quantities associated with fine-scale domain patterns (i.e., limiting local averages of strain and magnetization, and asymptotic distribution of their values in a neighborhood of an arbitrary material point) are discussed in Appendix A.2. In this simple example, all the asymptotic properties of the sequence are spatially homogeneous, but this will not be true in general. The physical meaning of Eq. (3.25) is that the supremum of $|\nabla \boldsymbol{y}^{(k)}|$ is uniformly bounded in Ω and in the limit $k \to \infty$, the sequence of deformations $\boldsymbol{y}^{(k)}$ can be approximated as closely as we wish by an affine deformation whose gradient is the weighted average of $\boldsymbol{F}_a$ and $\boldsymbol{F}_b$, in the sense that

$$\lim_{k\to\infty} \max_{\Omega} |\boldsymbol{y}^{(k)}(\boldsymbol{x}) - (\boldsymbol{c} + (\boldsymbol{I} + \boldsymbol{E}^{\infty})\boldsymbol{x})| = 0. \tag{3.26}$$

It is interesting to observe that, by modifying the sequence (3.17) in a small layer near the boundary of Ω, one may impose that, for every k,

$$\boldsymbol{y}^{(k)}(\boldsymbol{x}) = \boldsymbol{c} + (\boldsymbol{I} + \boldsymbol{E}^{\infty})\boldsymbol{x}, \quad \boldsymbol{x} \in \partial\Omega. \tag{3.27}$$

Using an argument similar to the one we will exploit in the proof of Theorem 4.1, one can construct such a modified sequence while keeping its asymptotic properties (3.22)–(3.24) unchanged. In particular, it has the same Young measure ν as the sequence constructed above. Therefore, if $(\boldsymbol{E}_a,\boldsymbol{m}_a)$ and $(\boldsymbol{E}_b,\boldsymbol{m}_b)$ belong to $\mathbb{K}$, the modified sequence satisfies the boundary condition (3.27) while giving rise to vanishing magnetoelastic energy, because

$$\operatorname{supp}\nu \subset \mathbb{K} \quad \text{a.e. in } \Omega. \tag{3.28}$$

Here, the boundary layer plays the role of a transition layer, i.e., a vanishingly small set where the state variables take values outside $\mathbb{K}$, and which does not contribute to the limiting energy.

To appreciate the crucial role played by transition layers, let's contrast the constraint (3.28) with the constraint that the state variables lie exactly on the energy wells everywhere in Ω:

$$\boldsymbol{E}[\boldsymbol{y}^k](\boldsymbol{x}) \in \{\boldsymbol{E}_a, \boldsymbol{E}_b\}, \quad \boldsymbol{x} \in \Omega, \quad k = 1, 2, \ldots \tag{3.29}$$

under the assumption that $\boldsymbol{E}_a \neq \boldsymbol{E}_b$. In this case, it is known that there are no sequences of deformations satisfying simultaneously Eq. (3.29) and the affine boundary condition $\boldsymbol{y}^{(k)}(\boldsymbol{x}) = \boldsymbol{c} + (\boldsymbol{I} + \boldsymbol{G})\boldsymbol{x}$, $\boldsymbol{x} \in \partial\Omega$ unless $\boldsymbol{G}$ is either equal to $\boldsymbol{E}_a$ or to $\boldsymbol{E}_b$. In these cases one has either $\boldsymbol{E}[\boldsymbol{y}^{(k)}](\boldsymbol{x}) = \boldsymbol{E}_a$ or $\boldsymbol{E}[\boldsymbol{y}^{(k)}](\boldsymbol{x}) = \boldsymbol{E}_b$ identically in Ω. By contrast, allowing the introduction of a boundary layer delivers a continuum of macroscopic average deformations of vanishing anisotropy energy.

These are obtained by satisfying Eq. (3.28) and matching the imposed boundary condition with any $\boldsymbol{G}$ of the form $\boldsymbol{G} = \lambda\boldsymbol{E}_a + (1-\lambda)\boldsymbol{E}_b$, and $\lambda \in [0,1]$.

4. The relaxed energy

4.1. Lower bound for the limiting energy: 'excess' energy and ellipsoidal samples

We are now ready to discuss the passage to the limit in Eq. (3.14). While the first two terms are linear, hence easily expressed in terms of the weak limits $(\boldsymbol{E}^{\infty}, \boldsymbol{m}^{\infty})$ of $(\boldsymbol{E}[\boldsymbol{y}^{(k)}], \boldsymbol{m}^{(k)})$, the limiting magnetostatic energy contains also a term which depends on some geometric features of the sequence, and which cannot be captured by the Young measure of $(\boldsymbol{E}[\boldsymbol{y}^{(k)}], \boldsymbol{m}^{(k)})$. In fact, denoting with 'Excess' this additional energy term, we have

$$\lim_{k\to\infty} \frac{1}{8\pi} \int_{\mathbb{R}^3} |\nabla\zeta_{\boldsymbol{m}^k}|^2 \,\mathrm{d}\boldsymbol{x} = \frac{1}{8\pi} \int_{\mathbb{R}^3} |\nabla\zeta_{\boldsymbol{m}^\infty}|^2 \,\mathrm{d}\boldsymbol{x} + \text{Excess}, \quad \text{Excess} \geqslant 0, \tag{4.1}$$

where, by definition, $\text{Excess} = \lim_{k\to\infty} \int |\nabla\zeta_{\boldsymbol{m}^k} - \nabla\zeta_{\boldsymbol{m}^\infty}|^2 \,\mathrm{d}\boldsymbol{x}$. Therefore, $\text{Excess} = 0$ if and only if

$$\nabla\zeta_{\boldsymbol{m}^k} \to \nabla\zeta_{\boldsymbol{m}^\infty} \text{ strongly in } L^2(\mathbb{R}^3). \tag{4.2}$$

For the simple laminate (3.18) it can be shown that (see James and Müller, 1994; DeSimone, 1996)

$$\text{Excess} = \frac{1}{8\pi} |\Omega| \, \lambda(1-\lambda) \, |(\boldsymbol{m}_b - \boldsymbol{m}_a)\cdot\boldsymbol{n}|^2. \tag{4.3}$$

Formulas (4.1) and (4.3) show that the limiting magnetostatic energy for a sequence like the one depicted in Fig. 2 consist of two terms. The first one could be called a 'macroscopic' term, since it depends on the magnetic 'phases' $\boldsymbol{m}_a$ and $\boldsymbol{m}_b$, and on their respective volume fractions λ, $(1-\lambda)$, only through the limiting local average $\boldsymbol{m}^{\infty}$. The second term is 'microscopic', in the sense that it is affected by the microgeometric features of the sequence of domain patterns $\boldsymbol{m}^{(k)}$, notably the relative orientation of the layer interfaces and of the magnetization vectors. In the magnetic jargon, Eq. (4.3) is the energy contribution due to the possible presence of internal poles, i.e., discontinuities across domain walls of the component of the magnetization orthogonal to the walls. For geometries more complicated than the one of Fig. 2, the term Excess in Eq. (4.1) can be evaluated using another measure associated with the sequence $\boldsymbol{m}^{(k)}$: the H-measure introduced by Tartar (see Tartar, 1990, 1995). In these circumstances, the precise mathematical condition ensuring that Eq. (4.1) holds with $\text{Excess} = 0$ is that $\operatorname{div} \boldsymbol{m}^{(k)}$ be compact in H^{-1}_{loc} (see Rogers, 1991; Pedregal, 1994; Tartar, 1995).

Exploiting the positivity of Excess is the first step towards finding a lower bound for the energy. Recalling (Appendix A.1) that the weak limit of $(\boldsymbol{E}[\boldsymbol{y}^{(k)}], \boldsymbol{m}^{(k)})$ is the center of mass of the corresponding Young measure $\nu_{\boldsymbol{x},\, \boldsymbol{x}\in\Omega}$, we have that $\operatorname{supp}\nu_{\boldsymbol{x}} \subset \mathbb{K}$ implies that there exist functions $\lambda_i \in L^2(\Omega)$, $0 \leqslant \lambda_i(\boldsymbol{x}) \leqslant 1$, $i = 1, \dots, N$ such that

$$\sum_{i=1}^{N} \lambda_i(\boldsymbol{x}) = 1 \quad \text{almost everywhere in } \Omega$$

and, in addition

$$\boldsymbol{E}^{\infty}(\boldsymbol{x}) = \sum_{i=1}^{N} \lambda_i(\boldsymbol{x})\boldsymbol{E}_i, \quad \boldsymbol{m}^{\infty}(\boldsymbol{x}) = \sum_{i=1}^{N} \lambda_i(\boldsymbol{x})\boldsymbol{m}_i. \tag{4.4}$$

Thus, with Eq. (4.1)

$$\lim_{k\to\infty} \left\{ -\int_{\Omega} (\boldsymbol{h}\cdot\boldsymbol{m}^{(k)} + \boldsymbol{S}\cdot\boldsymbol{E}[\boldsymbol{y}^{(k)}])\,\mathrm{d}\boldsymbol{x} + \frac{1}{8\pi}\int_{\mathbb{R}^3} |\nabla\zeta_{\boldsymbol{m}^{(k)}}|^2\,\mathrm{d}\boldsymbol{x} \right\} \geqslant \mathscr{E}^{\#}(\boldsymbol{E}^{\infty}, \boldsymbol{m}^{\infty}), \tag{4.5}$$

where

$$\mathscr{E}^{\#}(\boldsymbol{E}^{\infty}, \boldsymbol{m}^{\infty}) = -\int_{\Omega} (\boldsymbol{h}\cdot\boldsymbol{m}^{\infty}(\boldsymbol{x}) + \boldsymbol{S}\cdot\boldsymbol{E}^{\infty}(\boldsymbol{x}))\,\mathrm{d}\boldsymbol{x} + \frac{1}{8\pi}\int_{\mathbb{R}^3} |\nabla\zeta_{\boldsymbol{m}^{\infty}}(\boldsymbol{x})|^2\,\mathrm{d}\boldsymbol{x} \tag{4.6}$$

$$= -\left(\sum_{i=1}^{N} (\boldsymbol{h}\cdot\boldsymbol{m}_i + \boldsymbol{S}\cdot\boldsymbol{E}_i)\int_{\Omega} \lambda_i(\boldsymbol{x})\,\mathrm{d}\boldsymbol{x}\right) + \frac{1}{8\pi}\int_{\mathbb{R}^3} |\nabla\zeta_{\Sigma\lambda_i\boldsymbol{m}_i}(\boldsymbol{x})|^2\,\mathrm{d}\boldsymbol{x}. \tag{4.7}$$

Our second step towards the energy lower bound is based on a special property of ellipsoids, namely, that replacing a magnetization state with its average does not increase the magnetostatic energy (see Lemma A.1). Thus, assuming that Ω is an ellipsoid with demagnetizing matrix $\boldsymbol{D}$ (so that $-4\pi\boldsymbol{D}\boldsymbol{m}$ is the field induced in the interior of Ω by the constant magnetization $\boldsymbol{m}$, see Appendix A.1), we have

$$\frac{1}{8\pi}\int_{\mathbb{R}^3} |\nabla\zeta_{\Sigma\lambda_i\boldsymbol{m}_i}(\boldsymbol{x})|^2\,\mathrm{d}\boldsymbol{x} \geqslant \frac{1}{8\pi}\int_{\mathbb{R}^3} |\nabla\zeta_{\Sigma\langle\lambda_i\rangle\boldsymbol{m}_i}(\boldsymbol{x})|^2\,\mathrm{d}\boldsymbol{x} \tag{4.8}$$

$$= \frac{1}{2}|\Omega| \sum_{i,j=1}^{N} (\langle\lambda_j\rangle\boldsymbol{m}_j)\cdot 4\pi\boldsymbol{D}(\langle\lambda_i\rangle\boldsymbol{m}_i), \tag{4.9}$$

where $\langle\lambda_i\rangle$ is the average over Ω of the function λ_i

$$\langle\lambda_i\rangle = \frac{1}{|\Omega|}\int_{\Omega} \lambda_i(\boldsymbol{x})\,\mathrm{d}\boldsymbol{x} \in [0,1], \quad \sum_{i=1}^{N} \langle\lambda_i\rangle = 1 \tag{4.10}$$

and $|\Omega|$ is the volume of Ω. From Eqs. (4.6) and (4.8), it follows that for $\boldsymbol{E}^{\infty}$ and $\boldsymbol{m}^{\infty}$ given by Eq. (4.4) we have

$$\mathscr{E}^{\#}(\boldsymbol{E}^{\infty}, \boldsymbol{m}^{\infty}) \geqslant \mathscr{E}^{\star}(\langle\lambda_1\rangle, \dots, \langle\lambda_N\rangle), \tag{4.11}$$

where

$$\mathscr{E}^{\star}(\theta_1, \dots, \theta_N) = |\Omega| \left(\frac{1}{2}\sum_{i,j=1}^{N} \theta_j\boldsymbol{m}_j \cdot 4\pi\boldsymbol{D}\theta_i\boldsymbol{m}_i - \sum_{i=1}^{N} \theta_i(\boldsymbol{h}\cdot\boldsymbol{m}_i + \boldsymbol{S}\cdot\boldsymbol{E}_i) \right). \tag{4.12}$$

Using Eqs. (4.11) and (4.5) to bound the limiting energy (3.14) from below, and taking the infinum on both sides of the resulting inequality we obtain

$$\inf_{\mathscr{S}}\left(\lim_{k\to\infty}\mathscr{E}_k(\boldsymbol{E}[\boldsymbol{y}^k],\boldsymbol{m}^k)\right) \geqslant \inf_{\mathscr{T}}\mathscr{E}^\star(\theta_1,\ldots,\theta_N), \tag{4.13}$$

where

$$\mathscr{T}=\left\{(\theta_1,\ldots,\theta_N)\in\mathbb{R}^N\colon 0\leqslant\theta_i\leqslant 1,\sum_{i=1}^N\theta_i=1\right\}. \tag{4.14}$$

We have thus obtained a lower bound for the variational problem for sequences (3.14). However, this lower bound becomes sharp, i.e., Eq. (4.13) holds as an equality if we can show that for every admissible choice of θ_i, $i=1,\ldots,N$, we can find an admissible sequence $(\boldsymbol{E}[\boldsymbol{y}^{(k)}],\boldsymbol{m}^{(k)})$ whose limiting energy is exactly $\mathscr{E}^\star$. More explicitly, equality in Eq. (4.13) follows if we can show that for every point $(\boldsymbol{E}^\infty,\boldsymbol{m}^\infty)$ in the convex hull of $\mathbb{K}$, we can find a sequence $(\boldsymbol{E}[\boldsymbol{y}^{(k)}],\boldsymbol{m}^{(k)})\in\mathscr{S}$ such that $(\boldsymbol{E}[\boldsymbol{y}^{(k)}]\boldsymbol{m}^{(k)})\rightharpoonup(\boldsymbol{E}^\infty,\boldsymbol{m}^\infty)$ and Eq. (4.2) holds. In the next section, we show that this is indeed the case, provided that $\mathbb{K}$ consists of pairwise compatible magnetoelastic wells.

Remark. A natural question is the following. What is the correct formulation of the constrained theory for nonellipsoidal specimens? When $\mathbb{K}$ consists of pairwise compatible wells, we conjecture that the relaxed energy should be given by $\mathscr{E}^\#$, see Eq. (4.6). The correct state variables should thus be the local average strain $\boldsymbol{E}^\infty$ and the local average magnetization $\boldsymbol{m}^\infty$, subject to the constraints

$$(\boldsymbol{E}^\infty(\boldsymbol{x}),\boldsymbol{m}^\infty(\boldsymbol{x}))\in \text{conv }\mathbb{K}\text{ almost everywhere in }\Omega \tag{4.15}$$

where conv $\mathbb{K}$ is the convex hull of $\mathbb{K}$, and

$$\boldsymbol{E}^\infty=\boldsymbol{E}[\boldsymbol{y}^\infty] \tag{4.16}$$

for some $\boldsymbol{y}^\infty$, i.e., $\boldsymbol{E}^\infty$ is a kinematically compatible strain field. This opens the way to the interesting possibility of (sequences of) energy minimizing domain patterns whose asymptotic features are genuinely $\boldsymbol{x}$-dependent, i.e. variable from point to point within the specimen, as in the case of Fig. 1. This possibility could be effectively explored numerically. The associated numerical problem would be much simpler than the general micromagnetic problem. The missing technical step is, however, to prove that for every pair of fields $(\boldsymbol{E}^\infty,\boldsymbol{m}^\infty)$ satisfying Eqs. (4.15), (4.16)—together with the natural regularity requirements—one can find a sequence in $\mathscr{S}$ converging weakly to $(\boldsymbol{E}^\infty,\boldsymbol{m}^\infty)$ and whose energy is Eq. (4.6).

4.2. Attainment of the lower bound for the limiting energy

Theorem 4.1. *Assume that $\mathbb{K}$ consists of N pairwise compatible magnetoelastic wells. If $(\boldsymbol{E}^{(k)},\boldsymbol{m}^{(k)})\rightharpoonup(\boldsymbol{E}^\infty,\boldsymbol{m}^\infty)$ in $\mathscr{A}$ has Young measure $\nu_{\boldsymbol{x}}$ with* $\operatorname{supp}\nu_{\boldsymbol{x}}\subset\mathbb{K}$, *then $(\boldsymbol{E}^\infty,\boldsymbol{m}^\infty)$ belongs to the convex hull of $\mathbb{K}$.*

Conversely, let $(\boldsymbol{E}^\infty,\boldsymbol{m}^\infty)\in M^{3\times3}_{\text{sym}}\times\mathbb{R}^3$ be a (strain, magnetization) pair that belongs to the convex hull of $\mathbb{K}$. Then there is a sequence $(\boldsymbol{E}^{(k)},\boldsymbol{m}^{(k)})$ in $\mathscr{A}$ with

Young measure $v_{\boldsymbol{x}}$ *that satisfies*

$$\operatorname{supp} v_{\boldsymbol{x}} \subset \mathbb{K} \quad \text{almost everywhere in } \Omega \tag{4.17}$$

and has no excess magnetostatic energy

$$\nabla\zeta_{\boldsymbol{m}^{(k)}} \to \nabla\zeta_{\boldsymbol{m}^{\infty}} \quad \text{in } L^2(\mathbb{R}^3). \tag{4.18}$$

The sequence of deformations $\boldsymbol{y}^{(k)}$ *satisfying* $\boldsymbol{E}[\boldsymbol{y}^{(k)}] = \boldsymbol{E}^{(k)}$ *can be chosen such that*

$$\boldsymbol{y}^{(k)}(\boldsymbol{x}) \to (\boldsymbol{I} + \boldsymbol{E}^{\infty})\,\boldsymbol{x} \quad \textit{uniformly}. \tag{4.19}$$

Proof. The first assertion follows immediately from the fact that the center of mass of a distibution of positive masses lies in the convex hull of the support of the distribution. In the language of Young measures, since $v_{\boldsymbol{x}}$ is a probability measure, hence positive and with unit total mass, we have

$$(\boldsymbol{E}^{\infty}, \boldsymbol{m}^{\infty}) = \int_{\operatorname{supp} v_{\boldsymbol{x}} \subset \mathbb{K}} (\boldsymbol{G}, \boldsymbol{g})\, \mathrm{d}v_{\boldsymbol{x}}(\boldsymbol{G}, \boldsymbol{g}) \in \operatorname{conv} \mathbb{K}. \tag{4.20}$$

The converse is proved by an induction argument, involving the explicit construction of layered sequences. First, consider the case $N=2$. Let $(\boldsymbol{E}^{\infty}, \boldsymbol{m}^{\infty})$ belong to the convex hull of $\mathbb{K} = \{(\boldsymbol{E}_1, \boldsymbol{m}_1), (\boldsymbol{E}_2, \boldsymbol{m}_2)\}$ so that there exists $\lambda \in [0,1]$ such that $(\boldsymbol{E}^{\infty}, \boldsymbol{m}^{\infty}) = \lambda(\boldsymbol{E}_1, \boldsymbol{m}_1) + (1-\lambda)(\boldsymbol{E}_2, \boldsymbol{m}_2)$, and assume that $0 < \lambda < 1$ (for otherwise there is nothing to prove). The simple laminate consisting of sequences (3.17), (3.18), with $(\boldsymbol{E}_a, \boldsymbol{m}_a) = (\boldsymbol{E}_1, \boldsymbol{m}_1)$, $(\boldsymbol{E}_b, \boldsymbol{m}_b) = (\boldsymbol{E}_2, \boldsymbol{m}_2)$, and $\boldsymbol{n} = \boldsymbol{n}_{12}$ has the required properties: see Eqs. (3.22) –(3.25), while Eq. (4.18) follows from the assumption

$$(\boldsymbol{m}_2 - \boldsymbol{m}_1) \cdot \boldsymbol{n}_{21} = 0 \tag{4.21}$$

in view of Eqs. (4.1) and (4.3).

Assuming now that the theorem holds true for $N = M \geqslant 2$, let us prove it for $N = M + 1$. The idea here is to construct a 'laminate of laminates' i.e., to modulate in alternate layers two sequences, each of which has the desired properties (4.17)–(4.19) but 'mixes' only M of the $M+1$ energy wells, see Fig. 3(b). The existence of such sequences is guaranteed by the induction hypothesis.

To proceed, we first observe that $\boldsymbol{E}^{\infty} \in \operatorname{conv}\{\boldsymbol{E}_1, \ldots, \boldsymbol{E}_{M+1}\}$ can be written as $\boldsymbol{E}^{\infty} = \sum_{i=1}^{M+1} \lambda_i \boldsymbol{E}_i$, with $\lambda_i \geqslant 0$ and $\sum_{i=1}^{M+1} \lambda_i = 1$, but also as

$$\boldsymbol{E}^{\infty} = \kappa_1 \boldsymbol{E}_1 + \sum_{H=2}^{M} \kappa_H \prod_{l=1}^{H-1} (1-\kappa_l) \boldsymbol{E}_H + \prod_{l=1}^{M} (1-\kappa_l) \boldsymbol{E}_{M+1}. \tag{4.22}$$

Indeed, choosing $\kappa_1 = \lambda_1$ and

$$\kappa_l = \left\{ \begin{array}{ll} 0 & \text{if } \sum_{m=1}^{l-1} \lambda_m = 1 \\ \frac{\lambda_l}{1-\sum_{m=1}^{l-1} \lambda_m} & \text{otherwise} \end{array} \right\} \quad l = 2, \ldots, M \tag{4.23}$$

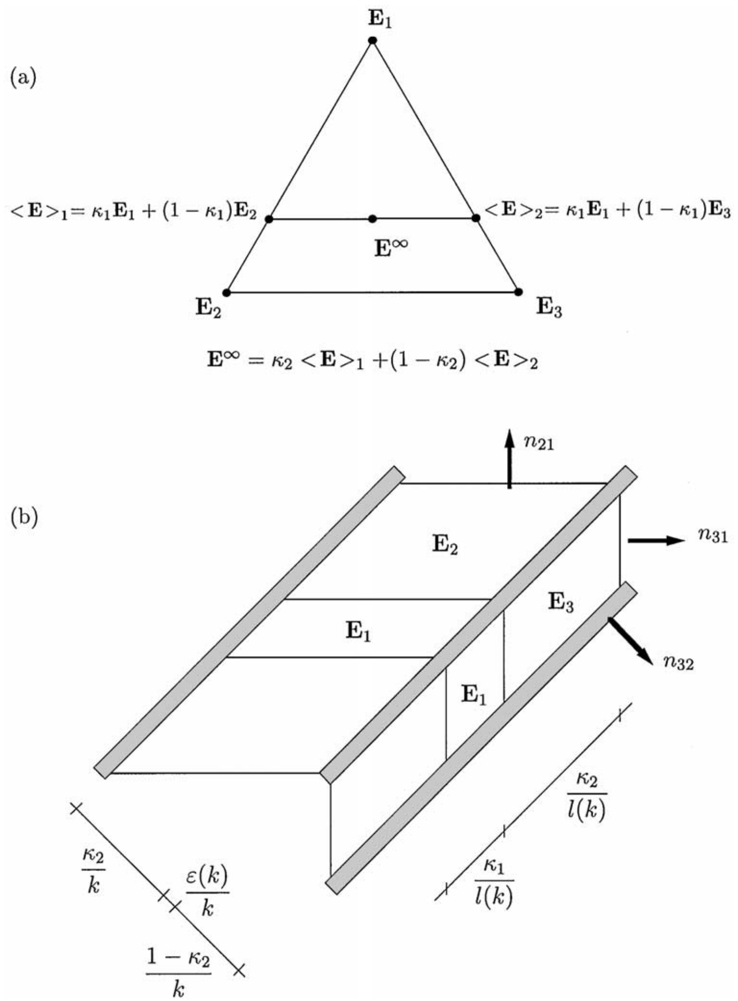

Fig. 3. (a) $\boldsymbol{E}^\infty$ arises by layering the compatible strains $\langle \boldsymbol{E}\rangle_1$ and $\langle \boldsymbol{E}\rangle_2$, which are in turn mixtures of the compatible strains $\boldsymbol{E}_1$, $\boldsymbol{E}_2$, and $\boldsymbol{E}_1$, $\boldsymbol{E}_3$, respectively; (b) a drawing of the corresponding laminate of laminates, showing also the transition layers.

we obtain that $\prod_{m=1}^{l-1}(1-\kappa_m) = 1 - \sum_{m=1}^{l-1}\lambda_m$ and therefore

$$\lambda_l = \kappa_l \prod_{m=1}^{l-1}(1-\kappa_m) \quad l = 2,\ldots,M, \tag{4.24}$$

$$\lambda_{M+1} = \prod_{m=1}^{M}(1-\kappa_m). \tag{4.25}$$

Thus, setting

$$\langle \boldsymbol{E}\rangle_1 = \kappa_1 \boldsymbol{E}_1 + \sum_{H=2}^{M-1} \kappa_H \prod_{l=1}^{H-1} (1-\kappa_l)\boldsymbol{E}_H + \prod_{l=1}^{M-1} (1-\kappa_l)\boldsymbol{E}_M, \tag{4.26}$$

$$\langle \boldsymbol{E}\rangle_2 = \kappa_1 \boldsymbol{E}_1 + \sum_{H=2}^{M-1} \kappa_H \prod_{l=1}^{H-1} (1-\kappa_l)\boldsymbol{E}_H + \prod_{l=1}^{M-1} (1-\kappa_l)\boldsymbol{E}_{M+1} \tag{4.27}$$

we have

$$\boldsymbol{E}^\infty = \kappa_M \langle \boldsymbol{E}\rangle_1 + (1-\kappa_M)\langle \boldsymbol{E}\rangle_2, \tag{4.28}$$

where $\langle \boldsymbol{E}\rangle_1$ and $\langle \boldsymbol{E}\rangle_2$ are kinematically compatible, since

$$\langle \boldsymbol{E}\rangle_2 - \langle \boldsymbol{E}\rangle_1 = \prod_{l=1}^{M-1} (1-\kappa_l)(\boldsymbol{E}_{M+1} - \boldsymbol{E}_M) = \frac{1}{2}(\boldsymbol{a}\otimes\boldsymbol{n} + \boldsymbol{n}\otimes\boldsymbol{a}) \tag{4.29}$$

in view of Eq. (2.13). Here, and in the remainder of the proof, we denote $\prod_{l=1}^{M-1}(1-\kappa_l)\boldsymbol{a}_{M+1,M}$ and $\boldsymbol{n}_{M+1,M}$ by $\boldsymbol{a}$, $\boldsymbol{n}$, respectively. Proceeding in the same manner for the magnetic variables, we have

$$\boldsymbol{m}^\infty = \kappa_M \langle \boldsymbol{m}\rangle_1 + (1-\kappa_M)\langle \boldsymbol{m}\rangle_2,$$

where the vectors

$$\langle \boldsymbol{m}\rangle_1 = \kappa_1 \boldsymbol{m}_1 + \sum_{H=2}^{M-1} \kappa_H \prod_{l=1}^{H-1} (1-\kappa_l)\boldsymbol{m}_H + \prod_{l=1}^{M-1} (1-\kappa_l)\boldsymbol{m}_M, \tag{4.30}$$

$$\langle \boldsymbol{m}\rangle_2 = \kappa_1 \boldsymbol{m}_1 + \sum_{H=2}^{M-1} \kappa_H \prod_{l=1}^{H-1} (1-\kappa_l)\boldsymbol{m}_H + \prod_{l=1}^{M-1} (1-\kappa_l)\boldsymbol{m}_{M+1} \tag{4.31}$$

satisfy the magnetic compatibility condition

$$(\langle \boldsymbol{m}\rangle_2 - \langle \boldsymbol{m}\rangle_1)\cdot \boldsymbol{n} = \prod_{l=1}^{M-1} (1-\kappa_l)(\boldsymbol{m}_{M+1} - \boldsymbol{m}_M)\cdot\boldsymbol{n} = 0 \tag{4.32}$$

in view of Eq. (2.14). Note that $(\langle \boldsymbol{E}\rangle_1, \langle \boldsymbol{m}\rangle_1)$ and $(\langle \boldsymbol{E}\rangle_2, \langle \boldsymbol{m}\rangle_2)$ are each in the convex hull of only M pairwise compatible wells.

Now, by the induction hypothesis, there exist sequences $(\boldsymbol{y}_1^{(l)}, \boldsymbol{m}_1^{(l)})$ and $(\boldsymbol{y}_2^{(l)}, \boldsymbol{m}_2^{(l)})$, with $(\boldsymbol{E}[\boldsymbol{y}_i^{(l)}], \boldsymbol{m}_i^{(l)})$ generating the Young measure $v_{i,\boldsymbol{x}}$, such that for $i=1,2$ we have

$$(\boldsymbol{E}[\boldsymbol{y}_i^{(l)}], \boldsymbol{m}_i^{(l)}) \rightharpoonup (\langle \boldsymbol{E}\rangle_i, \langle \boldsymbol{m}\rangle_i) \quad \text{in } \mathscr{A} \tag{4.33}$$

$$\nabla\zeta_{\boldsymbol{m}_i^{(l)}} \to \nabla\zeta_{\langle \boldsymbol{m}\rangle_i} \quad \text{in } L^2, \tag{4.34}$$

$$\operatorname{supp} v_{i,\boldsymbol{x}} \subset \mathbb{K}, \tag{4.35}$$

$$\boldsymbol{y}_i^{(l)}(\boldsymbol{x}) \to (\boldsymbol{I} + \langle \boldsymbol{E}\rangle_i)\boldsymbol{x} \text{ uniformly.} \tag{4.36}$$

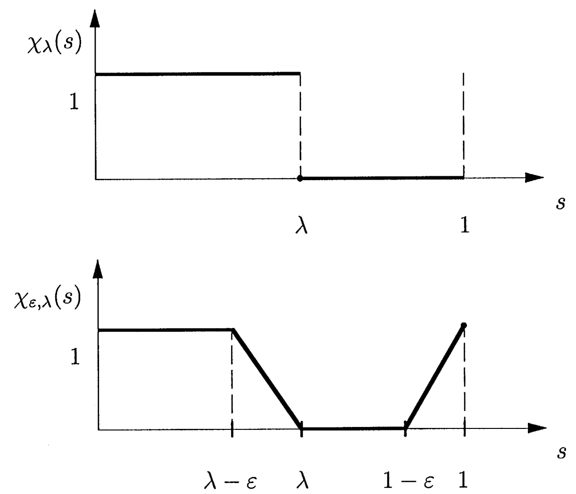

Fig. 4. The graphs of the functions χ_λ and $\chi_{\varepsilon,\lambda}$ used in the proof of Theorem 4.1.

Focusing on the magnetic variables first, set $\lambda = \kappa_M$, and define

$$\boldsymbol{m}^{(l,k)}(\boldsymbol{x}) = \chi_\lambda(k\boldsymbol{x}\cdot\boldsymbol{n})[\boldsymbol{m}_1^l(\boldsymbol{x})] + (1-\chi_\lambda(k\boldsymbol{x}\cdot\boldsymbol{n}))[\boldsymbol{m}_2^l(\boldsymbol{x})], \tag{4.37}$$

where χ_λ is given by Eq. (3.19) and has the graph shown in Fig. 4. Clearly

$$\begin{aligned}\boldsymbol{m}^{(l,k)}(\boldsymbol{x}) - \boldsymbol{m}^\infty = {} & \chi_\lambda(k\boldsymbol{x}\cdot\boldsymbol{n})[\boldsymbol{m}_1^{(l)}(\boldsymbol{x}) - \langle\boldsymbol{m}\rangle_1] \\ & + (1-\chi_\lambda(k\boldsymbol{x}\cdot\boldsymbol{n}))[\boldsymbol{m}_2^{(l)}(\boldsymbol{x}) - \langle\boldsymbol{m}\rangle_2] \\ & + [\chi_\lambda(k\boldsymbol{x}\cdot\boldsymbol{n})\langle\boldsymbol{m}\rangle_1 + (1-\chi_\lambda(k\boldsymbol{x}\cdot\boldsymbol{n}))\langle\boldsymbol{m}\rangle_2 - \boldsymbol{m}^\infty]\end{aligned}$$

or, setting $\tilde{\boldsymbol{m}}_i^{(l)}(\boldsymbol{x}) = \boldsymbol{m}_i^{(l)}(\boldsymbol{x}) - \langle\boldsymbol{m}\rangle_i$, $\Omega_1^k = \{\boldsymbol{x}\in\Omega\colon \chi_\lambda(k\boldsymbol{x}\cdot\boldsymbol{n}) = 1\}$, $\Omega_2^k = \{\boldsymbol{x}\in\Omega\colon \chi_\lambda(k\boldsymbol{x}\cdot\boldsymbol{n}) = 0\}$, $\tilde{\boldsymbol{m}}^{(k)}(\boldsymbol{x}) = [\chi_\lambda(k\boldsymbol{x}\cdot\boldsymbol{n})\langle\boldsymbol{m}\rangle_1 + (1-\chi_\lambda(k\boldsymbol{x}\cdot\boldsymbol{n}))\langle\boldsymbol{m}\rangle_2 - \boldsymbol{m}^\infty]$, we have that

$$\boldsymbol{m}^{(l,k)} - \boldsymbol{m}^\infty = \chi_{\Omega_1^k}\tilde{\boldsymbol{m}}_i^{(l)} + \chi_{\Omega_2^k}\tilde{\boldsymbol{m}}_2^{(l)} + \tilde{\boldsymbol{m}}^{(k)}. \tag{4.38}$$

Letting $l\to\infty$ with k fixed, we have that $\nabla\zeta_{\chi_{\Omega_i^k}\tilde{\boldsymbol{m}}_i^{(l)}} \to 0$ strongly in $L^2(\mathbb{R}^3)$, in view of Eq. (4.34) and of Lemma A.2. Thus, we can choose $l = l_1(k)$ such that

$$\|\nabla\zeta_{\chi_{\Omega_i^k}}\tilde{\boldsymbol{m}}_i^{(l_1(k))}\|_{L^2} < \frac{1}{k}, \quad i = 1,2 \tag{4.39}$$

and

$$\chi_{\Omega_i^k}\tilde{\boldsymbol{m}}_i^{(l_1(k))} \rightharpoonup 0 \quad \text{in } L^2. \tag{4.40}$$

The latter is slightly delicate mathematically, though clear from the physical viewpoint because of the separation of scales in ‘layers-within-layers’. The argument goes as follows. Clearly $\chi_{\Omega_i^k}\tilde{m}_i^{(l)} \rightharpoonup 0$ as $l\to\infty$ with k fixed. Multiply this function by a test function Ψ belonging to $\{\Psi_1, \Psi_2, \ldots\}$, a countable dense subset of L^2. For each Ψ_i there is a corresponding $l_i(k)$ that makes Eq. (4.39) hold. The diagonal sequence $l_k(k)$ then works for all of L^2, and by taking a further subsequence one can satisfy both Eqs. (4.39) and (4.40).

Now observe that $\tilde{\boldsymbol{m}}^{(k)}$ consists of simple layers, converges weakly to zero and, in view of Eqs. (4.3) and (4.32)

$$\lim_{k\to\infty} ||\nabla\zeta_{\tilde{\boldsymbol{m}}^{(k)}}||_{L^2} = 0.$$

Thus, by the linearity of the map $\boldsymbol{m} \mapsto \nabla\zeta_{\boldsymbol{m}}$, and the triangle inequality

$$\int_{\mathbb{R}^3} |\nabla\zeta_{\boldsymbol{m}^{(l_1(k),k)}}(\boldsymbol{x}) - \nabla\zeta_{\boldsymbol{m}^\infty}(\boldsymbol{x})|^2\,\mathrm{d}\boldsymbol{x}$$

$$= 9\int_{\mathbb{R}^3} \left|\frac{1}{3}(\nabla\zeta_{\chi_{\Omega_1^k}\tilde{\boldsymbol{m}}_1^{(l_1(k))}}(\boldsymbol{x}) + \nabla\zeta_{\chi_{\Omega_2^k}\tilde{\boldsymbol{m}}_2^{(l_1(k))}}(\boldsymbol{x}) + \nabla\zeta_{\tilde{\boldsymbol{m}}^{(k)}}(\boldsymbol{x}))\right|^2\,\mathrm{d}\boldsymbol{x}$$

$$\leqslant 3(||\nabla\zeta_{\chi_{\Omega_1^k}\tilde{\boldsymbol{m}}_1^{(l_1(k))}}||_{L^2}^2 + ||\nabla\zeta_{\chi_{\Omega_2^k}\tilde{\boldsymbol{m}}_2^{(l_1(k))}}||_{L^2}^2 + ||\nabla\zeta_{\tilde{\boldsymbol{m}}^{(k)}}||_{L^2}^2)$$

and the right-hand side tends to zero as $k \to \infty$ by Eqs. (4.38) and (4.39). Thus, in view of the decomposition (4.38), we have shown that $\boldsymbol{m}^{(l_1(k),k)} \rightharpoonup \boldsymbol{m}^\infty$ and $\nabla\zeta_{\boldsymbol{m}^{(k)}} \to \nabla\zeta_{\boldsymbol{m}^\infty}$ in L^2.

We turn now to the deformations. Setting $\tilde{\boldsymbol{y}}_i^{(l)}(\boldsymbol{x}) = \boldsymbol{y}_i^{(l)}(\boldsymbol{x}) + \boldsymbol{W}_i\boldsymbol{x}$, where

$$\boldsymbol{W}_1 = -\frac{\lambda}{2}(\boldsymbol{a}\otimes\boldsymbol{n} - \boldsymbol{n}\otimes\boldsymbol{a}), \tag{4.41}$$

$$\boldsymbol{W}_2 = \frac{(1-\lambda)}{2}(\boldsymbol{a}\otimes\boldsymbol{n} - \boldsymbol{n}\otimes\boldsymbol{a}) \tag{4.42}$$

we have, in view of Eq. (4.36), that

$$\boldsymbol{y}_i^{(l)} \to \langle\boldsymbol{F}\rangle_i\boldsymbol{x} \quad \text{uniformly as } l \to \infty, \tag{4.43}$$

where $\langle\boldsymbol{F}\rangle_i = \boldsymbol{I} + \langle\boldsymbol{E}\rangle_i + \boldsymbol{W}_i$, and

$$\langle\boldsymbol{F}\rangle_2 - \langle\boldsymbol{F}\rangle_1 = \boldsymbol{a}\otimes\boldsymbol{n}. \tag{4.44}$$

Extracting subsequences, if necessary, we can also assume that

$$\max_{\Omega}|\tilde{\boldsymbol{y}}_i^{(l)} - \langle\boldsymbol{F}\rangle_i\boldsymbol{x}| < \frac{1}{l}, \quad i = 1, 2. \tag{4.45}$$

For $0 < \varepsilon < \min\{\lambda, (1-\lambda)\}$, let $\chi_{\varepsilon,\lambda}$ be the 1-periodic function whose graph is given in Fig. 4, and define $\boldsymbol{y}_\varepsilon^{(l,k)} : \mathbb{R}^3 \to \mathbb{R}^3$ by

$$\boldsymbol{y}_\varepsilon^{(l,k)}(\boldsymbol{x}) = \chi_{\varepsilon,\lambda}(k\boldsymbol{x}\cdot\boldsymbol{n})\left[\tilde{\boldsymbol{y}}_1^{(l)}(\boldsymbol{x}) - \frac{1}{k}\boldsymbol{a}\int_0^{k\boldsymbol{x}\cdot\boldsymbol{n}}(\chi_{\varepsilon,\lambda}(s) - 1)\,\mathrm{d}s\right]$$

$$+ (1 - \chi_{\varepsilon,\lambda}(k\boldsymbol{x}\cdot\boldsymbol{n}))\left[\tilde{\boldsymbol{y}}_2^{(l)}(\boldsymbol{x}) - \frac{1}{k}\boldsymbol{a}\int_0^{k\boldsymbol{x}\cdot\boldsymbol{n}}\chi_{\varepsilon,\lambda}(s)\,\mathrm{d}s\right] \tag{4.46}$$

(cf. Fig. 4(b)), so that

$$\nabla \boldsymbol{y}_\varepsilon^{(l,k)}(\boldsymbol{x}) = \chi_{\varepsilon,\lambda}(k\boldsymbol{x}\cdot\boldsymbol{n})\nabla\tilde{\boldsymbol{y}}_1^{(l)}(\boldsymbol{x}) + (1-\chi_{\varepsilon,\lambda}(k\boldsymbol{x}\cdot\boldsymbol{n}))\nabla\tilde{\boldsymbol{y}}_2^{(l)}(\boldsymbol{x}) \\ - \{[\tilde{\boldsymbol{y}}_2^{(l)}(\boldsymbol{x}) - \tilde{\boldsymbol{y}}_1^{(l)}(\boldsymbol{x}) - (\boldsymbol{x}\cdot\boldsymbol{n})\boldsymbol{a}]k\chi'_{\varepsilon,\lambda}(k\boldsymbol{x}\cdot\boldsymbol{n})\}\otimes\boldsymbol{n}. \tag{4.47}$$

The last formula shows that $\nabla \boldsymbol{y}_\varepsilon^{(l,k)}(\boldsymbol{x})$ is equal to either $\nabla \boldsymbol{y}_1^{(l)}(\boldsymbol{x})$ (this happens on the set $\Omega^k_{1,\varepsilon} = \{\boldsymbol{x}\in\Omega\colon \chi_{\varepsilon,\lambda}(k\boldsymbol{x}\cdot\boldsymbol{n}) = 1\}$) or $\nabla \boldsymbol{y}_2^{(l)}(\boldsymbol{x})$ (this happens on the set $\Omega^k_{2,\varepsilon} = \{\boldsymbol{x}\in\Omega\colon \chi_{\varepsilon,\lambda}(k\boldsymbol{x}\cdot\boldsymbol{n}) = 0\}$), except on the set of the transition layers

$$\Omega^k_\varepsilon := \{\boldsymbol{x}\in\Omega\colon \chi'_{\varepsilon,\lambda}(k\boldsymbol{x}\cdot\boldsymbol{n}) \neq 0\} \tag{4.48}$$

whose measure is bounded by the product of the number of layers times their volume

$$\text{meas}\ \Omega^k_\varepsilon \leqslant (2k\ \text{diam}\ \Omega)\left(\pi\left(\frac{\text{diam}\ \Omega}{2}\right)^2\frac{\varepsilon}{k}\right) = \pi\frac{\text{diam}\ \Omega}{2}\varepsilon$$

(here diam Ω is the maximum diameter of Ω). Since Eqs. (4.44), (4.45) imply that $|\boldsymbol{y}_2^{(l)}(\boldsymbol{x}) - \boldsymbol{y}_1^{(l)}(\boldsymbol{x}) - (\boldsymbol{x}\cdot\boldsymbol{n})\boldsymbol{a}| \leqslant \frac{2}{l}$, we have that

$$|\nabla \boldsymbol{y}_\varepsilon^{(l,k)}(\boldsymbol{x})| \leqslant \max_{\boldsymbol{x}\in\Omega}\{|\nabla\tilde{\boldsymbol{y}}_1^{(l)}(\boldsymbol{x})|, |\nabla\tilde{\boldsymbol{y}}_2^{(l)}(\boldsymbol{x})|\} + \frac{2k}{l\varepsilon}. \tag{4.49}$$

We can then choose $l = l(k) = kl_1(k) \geqslant l_1(k)$, $\varepsilon = \varepsilon(k)$ such that $\varepsilon(k)\to 0$, and $k/l(k)\varepsilon(k) \leqslant 1$ (e.g., $l(k) = kl_1(k)$, $\varepsilon(k) = 1/l_1(k)$). It follows that $\nabla \boldsymbol{y}_{\varepsilon(k)}^{(l(k),k)}$ is uniformly bounded, and that meas $\Omega^k_{\varepsilon(k)} \to 0$. Thus, from the sequences $(\boldsymbol{y}^{(k)} = \boldsymbol{y}_{\varepsilon(k)}^{(l(k),k)}, \boldsymbol{m}^{(k)} = \boldsymbol{m}^{(l(k),k)})$ we can extract subsequences, not relabelled, such that $\boldsymbol{y}^{(k)} \to \boldsymbol{y}^\infty$ uniformly, $(\boldsymbol{E}[\boldsymbol{y}^{(k)}], \boldsymbol{m}^{(k)}) \rightharpoonup (\boldsymbol{E}^\infty, \boldsymbol{m}^\infty)$ in $\mathscr{A}$, Eq. (4.18) holds, and such that $(\boldsymbol{E}[\boldsymbol{y}^{(k)}], \boldsymbol{m}^{(k)})$ generates a Young measure $\nu_{\boldsymbol{x}}$. Our last step is to show that $\operatorname{supp}\nu_{\boldsymbol{x}} \subset \mathbb{K}$, and to identify $\boldsymbol{y}^\infty$ and $\boldsymbol{E}^\infty$.

Recalling definition (A.4) given in Appendix A.2, let $\Psi \in C^0(M^{3\times 3}_{\text{sym}}, \mathbb{R}^3)$ be a non-negative continuous function which vanishes exactly on $\mathbb{K}$ (i.e., $\Psi(\boldsymbol{G},\boldsymbol{g}) = 0$ if and only if $(\boldsymbol{G},\boldsymbol{g}) \in \mathbb{K}$) and which grows quadratically at infinity. Then

$$\int_\Omega\int_{M^{3\times 3}_{\text{sym}}\times\mathbb{R}^3} \Psi(\boldsymbol{G},\boldsymbol{g})\,\mathrm{d}\nu_{\mathrm{x}}(\boldsymbol{G},\boldsymbol{g}) = \lim_{k\to\infty}\int_\Omega \Psi(\boldsymbol{E}[\boldsymbol{y}^{(k)}](\boldsymbol{x}), \boldsymbol{m}^{(k)}(\boldsymbol{x}))\,\mathrm{d}\boldsymbol{x}$$

$$= \lim_{k\to\infty}\left\{\int_{\Omega^k_{1,\varepsilon(k)}} \Psi(\boldsymbol{E}[\boldsymbol{y}_1^{(l(k))}](\boldsymbol{x}), \boldsymbol{m}_1^{(l(k))}(\boldsymbol{x}))\,\mathrm{d}\boldsymbol{x}\right.$$

$$+ \int_{\Omega^k_{2,\varepsilon(k)}} \Psi(\boldsymbol{E}[\boldsymbol{y}_2^{(l(k))}](\boldsymbol{x}), \boldsymbol{m}_2^{(l(k))}(\boldsymbol{x}))\,\mathrm{d}\boldsymbol{x}$$

$$
\left. + \int_{\Omega^k_{\varepsilon(k)}} \Psi(\boldsymbol{E}[\boldsymbol{y}^{(k)}](\boldsymbol{x}), \boldsymbol{m}^{(k)}(\boldsymbol{x}))\,\mathrm{d}\boldsymbol{x} \right\}
$$

$$
\leqslant \lim_{k\to\infty} \left\{ \sum_{i=1}^{2} \int_{\Omega} \Psi(\boldsymbol{E}[\boldsymbol{y}_i^{(l(k))}](\boldsymbol{x}), \boldsymbol{m}_i^{(l(k))}(\boldsymbol{x}))\,\mathrm{d}\boldsymbol{x} \right\}
$$

$$
= \sum_{i=1}^{2} \int_{\Omega} \int_{\mathbb{K}} \Psi(\boldsymbol{G}, \boldsymbol{g})\,\mathrm{d}v_{i,\boldsymbol{x}}(\boldsymbol{G}, \boldsymbol{g})
$$

and since the right-hand side vanishes by Eq. (4.35), $\operatorname{supp} v_{\boldsymbol{x}} \subset \mathbb{K}$. Here we have used the fact that $\boldsymbol{m}^{(k)}$ and $\nabla \boldsymbol{y}^{(k)}$ (and hence of $\boldsymbol{E}[\boldsymbol{y}^{(k)}]$) are uniformly bounded, Ψ is continuous, and the measure of the transition layers $\Omega^k_{\varepsilon(k)}$ vanishes in the limit $k \to 0$.

Now we identify the limiting deformation and strain. From Eq. (4.46), using Eqs. (4.43) and (4.44), we have that

$$
\boldsymbol{y}^{(l(k),k)}_{\varepsilon(k)}(\boldsymbol{x}) = \chi_{\varepsilon(k),\lambda}(k\boldsymbol{x}\cdot\boldsymbol{n}) \left[\langle \boldsymbol{F} \rangle_2 \boldsymbol{x} - \frac{1}{k}\boldsymbol{a} \int_0^{k\boldsymbol{x}\cdot\boldsymbol{n}} \chi_{\varepsilon(k),\lambda}(\mathrm{s})\,\mathrm{d}s \right]
$$

$$
+ (1 - \chi_{\varepsilon(k),\lambda}(k\boldsymbol{x}\cdot\boldsymbol{n})) \left[\langle \boldsymbol{F} \rangle_2 \boldsymbol{x} - \frac{1}{k}\boldsymbol{a} \int_0^{k\boldsymbol{x}\cdot\boldsymbol{n}} \chi_{\varepsilon(k),\lambda}(\mathrm{s})\,\mathrm{d}s \right] + \boldsymbol{e}_k(\boldsymbol{x}),
$$

where

$$
\boldsymbol{e}_k(\boldsymbol{x}) = \chi_{\varepsilon(k),\lambda}(k\boldsymbol{x}\cdot\boldsymbol{n})[\boldsymbol{y}_1^{(l(k))}(\boldsymbol{x}) - \langle \boldsymbol{F} \rangle_1 \boldsymbol{x}]
$$

$$
+ (1 - \chi_{\varepsilon(k),\lambda}(k\boldsymbol{x}\cdot\boldsymbol{n}))[\boldsymbol{y}_2^{(l(k))}(\boldsymbol{x}) - \langle \boldsymbol{F} \rangle_2 \boldsymbol{x}]
$$

and we can assume $|\boldsymbol{e}_k(\boldsymbol{x})| \leqslant 2/l(k)$ in view of Eq. (4.45). Thus

$$
\boldsymbol{y}^{(l(k),k)}_{\varepsilon(k)}(\boldsymbol{x}) = \langle \boldsymbol{F} \rangle_2 \boldsymbol{x} - \frac{1}{k}\boldsymbol{a} \int_0^{k\boldsymbol{x}\cdot\boldsymbol{n}} \chi_{\varepsilon(k),\lambda}(\mathrm{s})\,\mathrm{d}s + \boldsymbol{e}_k(\boldsymbol{x})
$$

which (with a calculation similar to the one used to pass from Eqs. (3.17) to (3.20), since $\varepsilon(k) \to 0$) leads to $\boldsymbol{y}^{(k)} \to \boldsymbol{y}^{\infty} = \boldsymbol{F}^{\infty}\boldsymbol{x}$, where $\boldsymbol{F}^{\infty} = \lambda\langle \boldsymbol{F} \rangle_1 + (1-\lambda)\langle \boldsymbol{F} \rangle_2 = \boldsymbol{I} + \boldsymbol{E}^{\infty}$ in view of Eqs. (4.41), (4.42). This last result also implies that $\boldsymbol{E}[\boldsymbol{y}^{(k)}] \rightharpoonup \boldsymbol{E}^{\infty} = \boldsymbol{E}[\boldsymbol{y}^{\infty}]$ in $L^2(\Omega)$, and the proof is finished. □

Remark. Theorem 4.1 extends to the magnetoelastic case results of Bhattacharya (1993) and DeSimone (1993). It remains valid under the additional displacement boundary condition on $\boldsymbol{y}^{(k)}$

$$
\boldsymbol{y}^k(\boldsymbol{x})|_{\partial\Omega} = (\boldsymbol{I} + \boldsymbol{E}^{\infty})\boldsymbol{x}. \tag{4.50}
$$

In this case, the construction of $\boldsymbol{y}^{(k)}$ needs to be modified by introducing a boundary layer, so that Eq. (4.50) can be met. In fact, it can be shown (Ball and James, 1992) that this boundary layer behaves like a transition layer, contributing nothing to the limiting energy, or to the asymptotic distribution of the values of $\nabla \boldsymbol{y}^{(k)}$ or of $\boldsymbol{E}[\boldsymbol{y}^{(k)}]$.

4.3. Summary of the constrained theory: the relaxed energy

We summarize in this subsection the lengthy sequence of steps which has lead us from the energy functional of micromagnetics (2.11)

$$\mathscr{E}(\boldsymbol{E}[\boldsymbol{y}],\boldsymbol{m}) = \int_\Omega \Phi(\boldsymbol{E}[\boldsymbol{y}](\boldsymbol{x}),\boldsymbol{m}(\boldsymbol{x}))\,\mathrm{d}\boldsymbol{x}$$
$$- \int_\Omega (\boldsymbol{S}\cdot\boldsymbol{E}[\boldsymbol{y}](\boldsymbol{x}) + \boldsymbol{h}\cdot\boldsymbol{m}(\boldsymbol{x}))\,\mathrm{d}\boldsymbol{x} + \frac{1}{8\pi}\int_{\mathbb{R}^3}|\nabla\zeta_{\boldsymbol{m}}(\boldsymbol{x})|^2\,\mathrm{d}\boldsymbol{x}$$

to the relaxed energy (4.12)

$$\mathscr{E}^\star(\theta_1,\dots,\theta_N) = |\Omega|\left(\frac{1}{2}\sum_{i,j=1}^{N}\theta_j\boldsymbol{m}_j\cdot 4\pi\boldsymbol{D}\theta_i\boldsymbol{m}_i - \sum_{i=1}^{N}\theta_i(\boldsymbol{h}\cdot\boldsymbol{m}_i + \boldsymbol{S}\cdot\boldsymbol{E}_i)\right).$$

This last expression represents the minimal energy available to the system compatible with the requirement that, for $i=1,\dots,N$, the volume fraction with state variables in the ith energy well is equal to θ_i. Roughly speaking Eq. (4.12) is the energy the system will choose if it is given a chance to relax, hence the name 'relaxed' energy.

Our first step has been to magnify the magnetoelastic moduli. We have thus defined a new energy $\mathscr{E}_k$ by replacing Φ with $\Phi_k = k\Phi$ in Eq. (2.11). The study of the limiting behavior of low-energy configurations when the moduli become large has led us to consider the class $\mathscr{S}$ of sequences of deformations and magnetizations with asymptotic values on the energy wells $\mathbb{K}$. Indeed, by Theorem 3.1

$$\lim_k\left(\inf_{\mathscr{A}}\mathscr{E}_k\right) = \inf_{\mathscr{S}}\left(\lim_k\left(\frac{1}{8\pi}\int_{\mathbb{R}^3}|\nabla\zeta_{\boldsymbol{m}^{(k)}}|^2\,\mathrm{d}\boldsymbol{x} - \int_\Omega(\boldsymbol{S}\cdot\boldsymbol{E}[\boldsymbol{y}^{(k)}] + \boldsymbol{h}\cdot\boldsymbol{m}^{(k)})\,\mathrm{d}\boldsymbol{x}\right)\right) \tag{4.51}$$

cf. Eq. (3.14). A first lower bound to the energy of the system is arrived at by neglecting a nonnegative 'microscopic' energy item, called Excess in Eq. (4.1). In fact

$$\lim_k\left(\frac{1}{8\pi}\int_{\mathbb{R}^3}|\nabla\zeta_{\boldsymbol{m}^{(k)}}|^2\,\mathrm{d}\boldsymbol{x} - \int_\Omega(\boldsymbol{S}\cdot\boldsymbol{E}[\boldsymbol{y}^{(k)}] + \boldsymbol{h}\cdot\boldsymbol{m}^{(k)})\,\mathrm{d}\boldsymbol{x}\right) \geqslant \mathscr{E}^\#(\boldsymbol{E}^\infty,\boldsymbol{m}^\infty),$$

where $\boldsymbol{E}[\boldsymbol{y}^{(k)}] \rightharpoonup \boldsymbol{E}^\infty$, $\boldsymbol{m}^{(k)} \rightharpoonup \boldsymbol{m}^\infty$, and

$$\mathscr{E}^\#(\boldsymbol{E}^\infty,\boldsymbol{m}^\infty) = \frac{1}{8\pi}\int_{\mathbb{R}^3}|\nabla\zeta_{\boldsymbol{m}^\infty}(\boldsymbol{x})|^2\,\mathrm{d}\boldsymbol{x} - \int_\Omega(\boldsymbol{S}\cdot\boldsymbol{E}^\infty(\boldsymbol{x}) + \boldsymbol{h}\cdot\boldsymbol{m}^\infty(\boldsymbol{x}))\,\mathrm{d}\boldsymbol{x}$$

cf. Eqs. (4.5) and (4.6). However, for ellipsoidal specimens

$$\mathscr{E}^\#\left(\sum_{i=1}^{N}\lambda_i(\boldsymbol{x})\boldsymbol{E}_i, \sum_{i=1}^{N}\lambda_i(\boldsymbol{x})\boldsymbol{m}_i\right) \geqslant \mathscr{E}^\star(\langle\lambda_1\rangle,\dots,\langle\lambda_N\rangle), \tag{4.52}$$

where $\langle\lambda_i\rangle$ are the averages over Ω of the functions $\lambda_i(\boldsymbol{x})$ defining $\boldsymbol{E}^\infty$ and $\boldsymbol{m}^\infty$, see Eq. (4.4), and

$$\mathscr{E}^\star(\theta_i,\dots,\theta_N) = |\Omega|\left(\frac{1}{2}\sum_{i,j=1}^{N}\theta_j\boldsymbol{m}_j\cdot 4\pi\boldsymbol{D}\theta_i\boldsymbol{m}_i - \sum_{i=1}^{N}\theta_i(\boldsymbol{h}\cdot\boldsymbol{m}_i + \boldsymbol{S}\cdot\boldsymbol{E}_i)\right)$$

cf. Eq. (4.12). Thus

$$\lim_k \left(\frac{1}{8\pi} \int_{\mathbb{R}_3} |\nabla \zeta_{\boldsymbol{m}^{(k)}}|^2 \, \mathrm{d}\boldsymbol{x} - \int_\Omega (\boldsymbol{S} \cdot \boldsymbol{E}[\boldsymbol{y}^{(k)}] + \boldsymbol{h} \cdot \boldsymbol{m}^{(k)}) \, \mathrm{d}\boldsymbol{x} \right) \geqslant \inf_{\mathscr{T}} \mathscr{E},$$

where $\mathscr{T}$ describes the set of N-tuples of volume fractions, and by Eq. (4.51)

$$\lim_{k\to\infty} \left(\inf_{\mathscr{S}} \mathscr{E}_k \right) \geqslant \lim_{\mathscr{T}} \mathscr{E}^{\#}(\theta_1, \ldots, \theta_N).$$

In view of Theorem 4.1, however, for every choice $(\theta_1, \ldots, \theta_N)$ there are sequences of strains and magnetizations such that

$$\mathscr{E}_k(\boldsymbol{E}^{(k)}, \boldsymbol{y}^{(k)}) \to \mathscr{E}^{\star}(\theta_1, \ldots, \theta_N).$$

Thus, in fact

$$\lim_k \left(\inf_{\mathscr{S}} \mathscr{E}_n \right) = \inf_{\mathscr{T}} \mathscr{E}^{\star}(\theta_1, \ldots, \theta_N)$$

and we can study the finite dimensional minimization problem for the relaxed energy $\mathscr{E}^{\star}$ to gain insight on the asymptotic behavior of the minimizers of the infinite dimensional minimization problem for the energy $\mathscr{E}_k$.

5. Applications

5.1. The constrained optimization problem

The unknowns of the new constrained theory represent the weights θ_i, $i = 1, \ldots, 2n$, by which each of the energy wells contributes to an energy minimizing configuration, i.e., θ_i is the volume fraction of the specimen in which the state variables lie in the ith well. Set

$$\langle \boldsymbol{m} \rangle = \sum_{i=1}^{N} \theta_i \boldsymbol{m}_i = \sum_{i=1}^{n} (\theta_i - \bar{\theta}_i) \boldsymbol{m}_i, \tag{5.1}$$

$$\langle \boldsymbol{E} \rangle = \sum_{i=1}^{N} \theta_i \boldsymbol{E}_i = \sum_{i=1}^{n} (\theta_i + \bar{\theta}_i) \boldsymbol{E}_i, \tag{5.2}$$

where $\bar{\theta}_i = \theta_{n+i}$ denotes the volume fraction of the material for which the strain and magnetization take the value $(\boldsymbol{E}_i, -\boldsymbol{m}_i)$, $i = 1, \ldots, n$,. Dividing Eq. (4.12) by the volume of Ω, we can express the relaxed energy (per unit volume) of the system as

$$\frac{1}{2} \langle \boldsymbol{m} \rangle \cdot 4\pi \boldsymbol{D} \langle \boldsymbol{m} \rangle - \boldsymbol{h} \cdot \langle \boldsymbol{m} \rangle - \boldsymbol{S} \cdot \langle \boldsymbol{E} \rangle \tag{5.3}$$

i.e., as a function of the $N = 2n$ scalars $\theta_i, \bar{\theta}_i$, $i = 1, \ldots, n$. These quantities are only restricted by the relations

$$\theta_i \in [0, 1], \quad i = 1, \ldots, n, \tag{5.4}$$

$$\bar{\theta}_i \in [0,1], \quad i = 1,\ldots,n, \tag{5.5}$$

$$\sum_{i=1}^{n} \theta_i + \bar{\theta}_i = 1 \tag{5.6}$$

expressing the fact that the θ_i's are indeed volume fractions making up for the whole body.

All of the constraints (5.4)–(5.6) can be expressed through a set of linear inequalities or equalities. Since the energy (5.3) is quadratic in the θ_i's, the problem of finding energy-minimizing states in the constrained theory is one of quadratic programming. With the aim of solving this problem for arbitrary values of the loading parameters $\boldsymbol{h}$ and $\boldsymbol{S}$, the following change of variables proves expedient. We set

$$\delta_i = \theta_i - \bar{\theta}_i, \quad i = 1,\ldots,n, \tag{5.7}$$

$$\mu_i = \theta_i + \bar{\theta}_i, \quad i = 1,\ldots,n \tag{5.8}$$

and note that constraints (5.4)–(5.5) on the volume fractions $\theta_i, \bar{\theta}_i$ are equivalent to the following constraints on the variables δ_i, μ_i:

$$\tfrac{1}{2}(\delta_i + \mu_i) \in [0,1], \quad i = 1,\ldots,n, \tag{5.9}$$

$$\tfrac{1}{2}(-\delta_i + \mu_i) \in [0,1], \quad i = 1,\ldots,n, \tag{5.10}$$

$$\sum_{i=1}^{n} \mu_i = 1. \tag{5.11}$$

Moreover, we let

$$\boldsymbol{A} = \left[\begin{array}{c|c} 4\pi \boldsymbol{m}_i \cdot \boldsymbol{D}\boldsymbol{m}_j & \boldsymbol{0} \\ \hline \boldsymbol{0} & \boldsymbol{0} \end{array}\right] \in M^{2n\times 2n}, \tag{5.12}$$

$$\boldsymbol{b}(\boldsymbol{h},\boldsymbol{S}) = \left[\begin{array}{c} \boldsymbol{h}\cdot\boldsymbol{m}_1 \\ \cdots \\ \boldsymbol{h}\cdot\boldsymbol{m}_n \\ \hline 0 \\ \cdots \\ 0 \end{array}\right] + \left[\begin{array}{c} 0 \\ \cdots \\ 0 \\ \hline \boldsymbol{S}\cdot\boldsymbol{E}_1 \\ \cdots \\ \boldsymbol{S}\cdot\boldsymbol{E}_n \end{array}\right], \quad \boldsymbol{x} = \left[\begin{array}{c} \delta_1 \\ \cdots \\ \delta_n \\ \hline \mu_1 \\ \cdots \\ \mu_n \end{array}\right], \tag{5.13}$$

$$\boldsymbol{C} = \frac{1}{2}\left[\begin{array}{c|c} \boldsymbol{I} & \boldsymbol{I} \\ \hline -\boldsymbol{I} & -\boldsymbol{I} \\ \hline -\boldsymbol{I} & \boldsymbol{I} \\ \hline \boldsymbol{I} & -\boldsymbol{I} \end{array}\right] \in M^{4n\times 2n}, \quad \boldsymbol{d} = \left[\begin{array}{c} 1 \\ \hline \mathrm{O} \\ \hline 1 \\ \hline \mathrm{O} \end{array}\right] \in M^{4n\times 1}, \tag{5.14}$$

$$\boldsymbol{G} = [0 \quad \cdots \quad 0 \mid 1 \quad \cdots \quad 1] \in M^{1\times 2n}, \quad \boldsymbol{f} = [1], \tag{5.15}$$

where $\mathbf{0}$, $\boldsymbol{I} \in M^{n\times n}$ are the zero and the identity $n \times n$ matrices, respectively, while O, $1 \in M^{n\times 1}$ are the column vectors with all entries equal to zero, or to one, respectively.

The energy-minimizing states of our system corresponding to the applied prestress $\boldsymbol{S}$ and applied magnetic field $\boldsymbol{h}$ are then the solutions of the following quadratic programming problem.

Problem QP. *Minimize*

$$\frac{1}{2}\boldsymbol{x}^{\mathrm{T}}\boldsymbol{A}\boldsymbol{x} - \boldsymbol{b}^{\mathrm{T}}(\boldsymbol{S},\boldsymbol{h})\boldsymbol{x} \tag{5.16}$$

among $\boldsymbol{x} \in \mathbb{R}^{2n}$ *such that*

$$\boldsymbol{C}\boldsymbol{x} \leqslant \boldsymbol{d} \quad \textit{and} \quad \boldsymbol{G}x = \boldsymbol{f}.$$

We may seek solutions to Problem QP by looking for Lagrange multipliers

$$\boldsymbol{\Lambda} = \begin{bmatrix} \lambda_1 \\ \vdots \\ \lambda_{4n} \end{bmatrix}, \quad \boldsymbol{\Lambda}' = [\lambda]$$

satisfying the Kuhn–Tucker optimality conditions

$$\boldsymbol{A}\boldsymbol{x} + \boldsymbol{C}^{\mathrm{T}}\boldsymbol{\Lambda} + \boldsymbol{G}^{\mathrm{T}}\boldsymbol{\Lambda}' = \boldsymbol{b}, \tag{5.17}$$

$$\lambda_j \geqslant 0, \quad \lambda_j\left(\sum_{i=1}^{2n}\boldsymbol{C}_{ji}x_i - d_j\right) = 0, \quad j = 1,\ldots,4n \tag{5.18}$$

and the requirement that the quadratic form $\boldsymbol{z}^{\mathrm{T}}\boldsymbol{A}z$ be positive-definite for $\boldsymbol{z}$ lying in the tangent space to the manifold of the active constraints for the solution point $\boldsymbol{x}$.

An alternative strategy to search for solutions to Problem QP is to take advantage of the special structure (5.12), (5.13) of the matrices $\boldsymbol{A}$, $\boldsymbol{b}$. For this purpose, define the column vectors $\boldsymbol{\mu} = (\mu_1,\ldots,\mu_n)$, $\boldsymbol{\delta} = (\delta_1,\ldots,\delta_n)$, $\tilde{\boldsymbol{h}} = (\boldsymbol{h}\cdot\boldsymbol{m}_1,\ldots,\boldsymbol{h}\cdot\boldsymbol{m}_n)$, $\tilde{\boldsymbol{S}} = (\boldsymbol{S}\cdot\boldsymbol{E}_1,\ldots,\boldsymbol{S}\cdot\boldsymbol{E}_n)$, and the $n\times n$ matrix $\tilde{\boldsymbol{D}}$ with components $\tilde{D}_{ij} = 4\pi\boldsymbol{D}\boldsymbol{m}_i\cdot\boldsymbol{m}_j$. With this notation, we can write the minimum of Eq. (5.3) as

$$\begin{aligned}
&\min_{\boldsymbol{\delta}\in\mathscr{B},\boldsymbol{\mu}\in\mathscr{C}}\left\{-\tilde{\boldsymbol{S}}\cdot\boldsymbol{\mu} - \tilde{\boldsymbol{h}}\cdot\boldsymbol{\delta} + \frac{1}{2}\boldsymbol{\delta}\cdot\tilde{\boldsymbol{D}}\boldsymbol{\delta}\right\}\\
&\quad=\min_{\boldsymbol{\delta}\in\mathscr{B}}\left\{-\min_{\boldsymbol{\mu}\in\mathscr{C}(\delta)}(\tilde{\boldsymbol{S}}\cdot\boldsymbol{\mu}) - \tilde{\boldsymbol{h}}\cdot\boldsymbol{\delta} + \frac{1}{2}\boldsymbol{\delta}\cdot\tilde{\boldsymbol{D}}\boldsymbol{\delta}\right\},
\end{aligned} \tag{5.19}$$

where the constraint sets $\mathscr{B},\mathscr{C},\mathscr{C}(\delta)$ appearing above are defined as follows:

$$\mathscr{B}:=\{\boldsymbol{\delta}\in\mathbb{R}^n:\ \exists \text{ a solution } (\boldsymbol{\mu},\boldsymbol{\delta})\in\mathbb{R}^{2n} \text{ of Eqs. (5.9)–(5.11)}\}$$

$$\mathscr{C}:=\{\boldsymbol{\mu}\in\mathbb{R}^n:\ \exists \text{ a solution } (\boldsymbol{\mu},\boldsymbol{\delta})\in\mathbb{R}^{2n} \text{ of Eqs. (5.9)–(5.11)}\}$$

$$\mathscr{C}(\boldsymbol{\delta}):=\{\boldsymbol{\mu}\in\mathbb{R}^n:\ \text{Eqs. (5.9)–(5.11) are satisfied for } (\boldsymbol{\mu},\boldsymbol{\delta}), \boldsymbol{\delta}\in\mathscr{B}\}.$$

Note that, for each $\boldsymbol{\delta} \in \mathscr{B}$, $\mathscr{C}(\boldsymbol{\delta})$ is a map of $\mathscr{B}$ into $\mathbb{R}^n$. Our strategy will then be that of minimizing out $\mu_1, \ldots, \mu_n$ first, by solving a problem of linear programming in which $\boldsymbol{\delta}$ is a vector of parameters, and then proceed with the outer minimization over fewer variables. Determining the constraint sets $\mathscr{B}$, $\mathscr{C}(\boldsymbol{\delta})$ is the crucial part of this calculation.

Lemma 5.1.

$$\mathscr{B} = \left\{ \boldsymbol{\delta} \in \mathbb{R}^n \colon \sum_{i=1}^{n} |\delta_i| \leqslant 1 \right\}. \tag{5.20}$$

$$\mathscr{C}(\boldsymbol{\delta}) = \left\{ \boldsymbol{\mu} \in \mathbb{R}^n \colon \mu_i \geqslant |\delta_i| \quad \text{and} \quad \sum_{i=1}^{n} \mu_i = 1 \right\}. \tag{5.21}$$

Proof. To prove Eq. (5.20), we note that Eqs. (5.9) and (5.10) imply that $-1 \leqslant \delta_i \leqslant 1$ and $\mu_i \geqslant |\delta_i|$. Hence

$$\sum_{i=1}^{n} |\delta_i| \leqslant \sum_{i=1}^{n} \mu_i = 1.$$

Conversely, suppose $\sum_{i=1}^{n} |\delta_i| \leqslant 1$. By continuity there exist $\mu_1, \ldots, \mu_n$ such that

$$|\delta_i| \leqslant \mu_i \leqslant 1, \quad i = 1, \ldots, n \tag{5.22}$$

and

$$\sum_{i=1}^{n} \mu_i = 1. \tag{5.23}$$

Also, Eq. (5.22) implies that $\mu_i \geqslant \delta_i$, $\mu_i \geqslant -\delta_i$, and, in turn, that $\mu_i + \delta_i \in [0, 2]$, $\mu_i - \delta_i \in [0, 2]$ which gives Eqs. (5.9), (5.10). Finally Eq. (5.21) is immediate from Eqs. (5.22), (5.23). □

Remark. There are many possible parametrizations of $\mathscr{C}(\boldsymbol{\delta})$, e.g.

$$\mu_i = |\delta_i| + \varepsilon_i, \quad i = 1, \ldots, n,$$

where $\varepsilon_i \geqslant 0$, and

$$\sum_{i=1}^{n} \varepsilon_i = 1 - \sum_{i=1}^{n} |\delta_i|.$$

It is also worth noticing that, since the constraints defining the set $\mathscr{B}$ are nonlinear, Eq. (5.19) is no longer a problem of quadratic programming. However, the procedure just outlined is often quite simple to implement.

5.2. Magnetostriction curves in Terfenol-D

We consider a single crystal of Terfenol-D, and we use as reference frame the one defined by the cubic axes of the material's undistorted crystalline lattice. We take Ω to

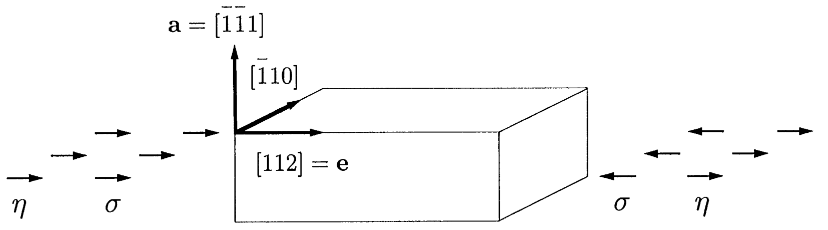

Fig. 5. The geometry of the Terfenol-D plate.

be an infinite slab, with faces orthogonal to the $[11\bar{1}]$ direction, so that its demagnetizing tensor $\boldsymbol{D}$ is given by

$$\boldsymbol{D} = \boldsymbol{a} \otimes \boldsymbol{a} \tag{5.24}$$

with $\boldsymbol{a}$ the unit vector $(-1,-1,1)/\sqrt{3}$, see Fig. 5. While our model is for single crystals, we note that a typical polycrystalline Terfenol-D specimens consists of parallel lamellae with every other slab having the orientation chosen here (see Clark, 1992).

The easy axes are along the [1 1 1] directions

$$\begin{aligned}
\pm\boldsymbol{m}_1 &= \pm\frac{m_\mathrm{s}}{\sqrt{3}}(1,\ 1,\ 1),\\
\pm\boldsymbol{m}_2 &= \pm\frac{m_\mathrm{s}}{\sqrt{3}}(-1,\ 1,\ 1),\\
\pm\boldsymbol{m}_3 &= \pm\frac{m_\mathrm{s}}{\sqrt{3}}(1,-1,\ 1),\\
\pm\boldsymbol{m}_4 &= \pm\frac{m_\mathrm{s}}{\sqrt{3}}(1,\ 1,-1) = \mp m_\mathrm{s}a
\end{aligned} \tag{5.25}$$

while the preferred strains are given by

$$\boldsymbol{E}_0(\boldsymbol{m}_i) = \boldsymbol{E}_i = \frac{3}{2}\lambda_{111}\left(\tilde{\boldsymbol{m}}_i \otimes \tilde{\boldsymbol{m}}_i - \frac{1}{3}\mathbf{1}\right), \quad i = 1,\dots,4. \tag{5.26}$$

Here $\lambda_{111} = 2\times10^{-3}$, $m_\mathrm{s} = 800\,\mathrm{emu/cm^3}$ is the saturation magnetization at room temperature, and $\tilde{\boldsymbol{m}}_i = \boldsymbol{m}_i/m_\mathrm{s}$.

For Terfenol-D, the energy wells $\mathbb{K} = \bigcup_{i=1}^4\{(\boldsymbol{E}_i, \pm\boldsymbol{m}_i)$ are pairwise compatible. Indeed, for a suitable scalar constant α we have

$$\begin{aligned}
\boldsymbol{E}_j - \boldsymbol{E}_k &= \frac{3}{2}\lambda_{111}(\tilde{\boldsymbol{m}}_j \otimes \tilde{\boldsymbol{m}}_j - \tilde{\boldsymbol{m}}_k \otimes \tilde{\boldsymbol{m}}_k)\\
&= \frac{\alpha}{2}\left(\frac{\boldsymbol{m}_j + \boldsymbol{m}_k}{|\boldsymbol{m}_j + \boldsymbol{m}_k|} \otimes \frac{\boldsymbol{m}_j - \boldsymbol{m}_k}{|\boldsymbol{m}_j - \boldsymbol{m}_k|} + \frac{\boldsymbol{m}_j - \boldsymbol{m}_k}{|\boldsymbol{m}_j - \boldsymbol{m}_k|} \otimes \frac{\boldsymbol{m}_j + \boldsymbol{m}_k}{|\boldsymbol{m}_j + \boldsymbol{m}_k|}\right)
\end{aligned}$$

and it is kinematically admissible to form an interface between the phases $(\boldsymbol{E}_j, \pm\boldsymbol{m}_j)$ and $(\boldsymbol{E}_k, \pm\boldsymbol{m}_k)$ with normal $\boldsymbol{n} = (\boldsymbol{m}_j + \boldsymbol{m}_j)/(|\boldsymbol{m}_j + \boldsymbol{m}_k|)$ which satisfies the magnetic compatibility condition

$$\pm(\boldsymbol{m}_j - \boldsymbol{m}_k) \cdot \boldsymbol{n} = 0$$

On the other hand, for an interface between phases $(\boldsymbol{E}_j, \pm\boldsymbol{m}_j)$ and $(\boldsymbol{E}_k, \mp\boldsymbol{m}_k)$ we can use the normal $\boldsymbol{n} = (\boldsymbol{m}_j + \boldsymbol{m}_k)/(|\boldsymbol{m}_j + \boldsymbol{m}_k|)$, so that the condition

$$\pm(\boldsymbol{m}_j + \boldsymbol{m}_k) \cdot \boldsymbol{n} = 0$$

is satisfied.

We assume that Ω is subjected to the compressive prestress $\boldsymbol{S}$ and to the applied magnetic field $\boldsymbol{h}$ given by

$$\boldsymbol{S} = -\sigma \boldsymbol{e} \otimes \boldsymbol{e}, \ \ \sigma \geqslant 0, \quad \boldsymbol{h} = \eta \boldsymbol{e}, \ \ \eta \geqslant 0, \tag{5.27}$$

where $\boldsymbol{e}$ is the unit vector $\boldsymbol{e} = (1,\ 1,\ 2)/\sqrt{6}$. With the notation of Section 5, we have

$$\boldsymbol{A} = \frac{4\pi m_s^2}{9} \left[\begin{array}{cccc|c} 1 & -1 & -1 & 3 & \\ -1 & 1 & 1 & -3 & \\ -1 & 1 & 1 & -3 & \mathbf{0} \\ 3 & -3 & -3 & 9 & \\ \hline & \mathbf{0} & & & \mathbf{0} \end{array} \right], \tag{5.28}$$

$$\boldsymbol{b}(\eta, \sigma) = \frac{2m_s}{3\sqrt{2}} \eta \begin{bmatrix} 2 \\ 1 \\ 1 \\ 0 \\ \hline 0 \\ 0 \\ 0 \\ 0 \end{bmatrix} - \frac{\lambda_{111}}{3} \sigma \begin{bmatrix} 0 \\ 0 \\ 0 \\ 0 \\ \hline 4 \\ 1 \\ 1 \\ 0 \end{bmatrix}, \quad \boldsymbol{x} = \begin{bmatrix} \delta_1 \\ \delta_2 \\ \delta_3 \\ \delta_4 \\ \hline \mu_1 \\ \mu_2 \\ \mu_3 \\ \mu_4 \end{bmatrix} \tag{5.29}$$

and we study the following magneto-mechanical loading program: for a given value of the prestress σ, consider the one-parameter family $\eta \mapsto \boldsymbol{x}_{\sigma,\eta}$ of solutions of Problem QP obtained by increasing the field strength η from zero to infinity. We take $\sigma = 11$ MPa in order to make a comparison between the predictions of our theory and the experimental observations of Teter et al. (1990) reproduced in Fig. 6. Table 1 summarizes our results for the solution vectors $\boldsymbol{x}_{\sigma,\eta}$, where the functions $\eta \mapsto \bar{\alpha}(\eta)$ and $\eta \mapsto \bar{\beta}(\eta)$ are given by

$$\bar{\alpha}(\eta) = \frac{3}{4} + \left(\eta - \frac{1}{\sqrt{2}} \frac{\lambda_{111}\sigma}{m_s} \right) \frac{3}{8 m_s \sqrt{2}},$$

$$\bar{\beta}(\eta) = \frac{1}{2} + \left(\eta - \frac{3}{\sqrt{2}} \frac{\lambda_{111}\sigma}{m_s} \right) \frac{3}{8 m_s \sqrt{2}}.$$

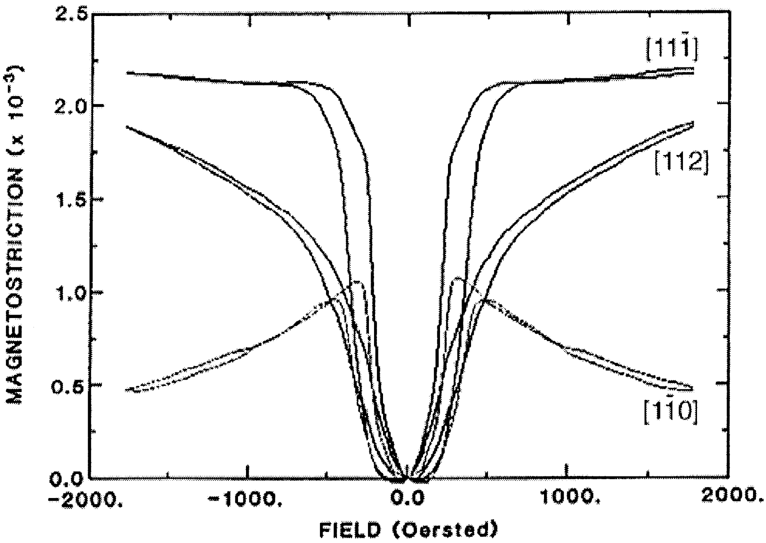

Fig. 6. Magnetostriction vs. applied magnetic field for three orthogonal crystallographic directions in $Tb_{0.3}Dy_{0.7}Fe_{1.95}$. The [11$\bar{2}$] data are along the crystal growth direction and are positive in sign. The [1 1 1] data are negative in sign while the [1$\bar{1}$0] are positive. Reprinted with permission from Teter et al., J. Appl. Phy. 67 (1990) 5005. © *1990 American Institute of Physics.*

Table 1
$\sigma = 11$ MPa

$\boldsymbol{x}_{\sigma,\eta}$	$\begin{bmatrix}0\\0\\0\\0\\0\\0\\0\\1\end{bmatrix}$	$\begin{bmatrix}0\\\alpha/2\\\alpha/2\\\alpha/3\\0\\\alpha/2\\\alpha/2\\1-\alpha\end{bmatrix}$	$\begin{bmatrix}0\\\bar{\alpha}(\eta)/2\\\bar{\alpha}(\eta)/2\\1-\bar{\alpha}(\eta)\\0\\\bar{\alpha}(\eta)/2\\\bar{\alpha}(\eta)/2\\1-\bar{\alpha}(\eta)\end{bmatrix}$	$\begin{bmatrix}\bar{\beta}(\tau)\\(1-\bar{\beta}(\tau))/2\\(1-\bar{\beta}(\tau))/2\\0\\\bar{\beta}(\tau)\\(1-\bar{\beta}(\tau))/2\\(1-\bar{\beta}(\tau))/2\\0\end{bmatrix}$	$\begin{bmatrix}1\\0\\0\\0\\1\\0\\0\\0\end{bmatrix}$
		$0 \leqslant \alpha \leqslant \frac{3}{4}$	$\frac{3}{4} \leqslant \bar{\alpha}(\eta) \leqslant \bar{\alpha}(\eta^*)$	$\bar{\beta}(\eta^*) \leqslant \bar{\beta}(\eta) \leqslant 1$	
Field strength	$0 \leqslant \eta \leqslant \frac{\lambda_{111}\sigma}{\sqrt{2}m_s}$	$\eta = \frac{\lambda_{111}\sigma}{\sqrt{2}m_s}$	$\frac{\lambda_{111}\sigma}{\sqrt{2}m_s} \leqslant \eta \leqslant \eta^*$ $:= \frac{7}{3}\frac{\lambda_{111}\sigma}{\sqrt{2}m_s}$	$\eta^* \leqslant \eta \leqslant 3\frac{\lambda_{111}\sigma}{\sqrt{2}m_s}$ $+ \frac{\sqrt{2}}{3}m_s$	$\eta \geqslant 3\frac{\lambda_{111}\sigma}{\sqrt{2}m_s}$ $+ \frac{\sqrt{2}}{3}m_s$

From the components $\delta_i(\eta), \mu_i(\eta)$ of the solution vectors $\boldsymbol{x}_{\sigma,\eta}$ we obtain the magnetostriction curves of Fig. 7 by plotting the following functions

$$\varepsilon_{112}(\eta) = \sum_{i=1}^{4} \mu_i(\eta)\boldsymbol{E}_i \cdot \boldsymbol{e} \otimes \boldsymbol{e},$$

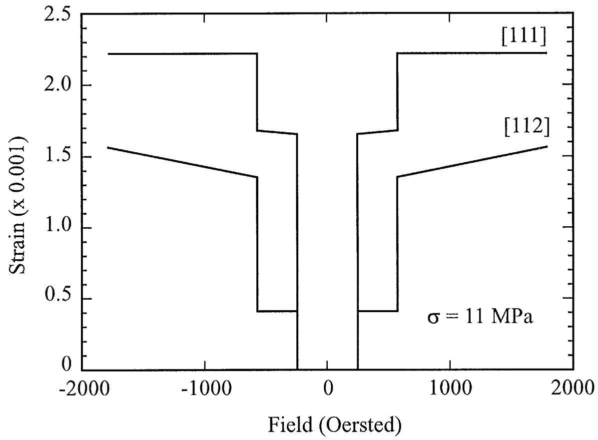

Fig. 7. Computed curves for the single crystal slab of Terfenol-D.

$$\bar{\varepsilon}_{11\bar{1}}(\eta) = -\varepsilon_{11\bar{1}}(\eta) = -\sum_{i=1}^{4} \mu_i(\eta)\boldsymbol{E}_i \cdot \boldsymbol{e}_\perp \otimes \boldsymbol{e}_\perp,$$

$$\varepsilon_{1\bar{1}0}(\eta) = \sum_{i=1}^{4} \mu_i(\eta)\boldsymbol{E}_i \cdot \boldsymbol{e}^\perp \otimes \boldsymbol{e}^\perp,$$

where $\boldsymbol{e}_\perp = \frac{1}{\sqrt{3}}(1,1,-1)$, $\boldsymbol{e}^\perp = \frac{1}{\sqrt{2}}(1,-1,1)$. We remark that since the $\boldsymbol{E}_i$'s have null trace, $\varepsilon_{1\bar{1}0}(\eta) + \varepsilon_{112}(\eta) = \bar{\varepsilon}_{11\bar{1}}(\eta)$ for all $\eta \in (0,\infty)$, and we have thus omitted the plot of the $1\bar{1}0$ magnetostriction curve. Moreover, we have chosen to plot $\bar{\varepsilon}_{11\bar{1}}(\eta)$ rather than $\varepsilon_{11\bar{1}}(\eta)$ to ease the comparison with the curves measured by Teter et al. (1990), reproduced in Fig. 6. We caution that the specimen used in these tests probably contained several parallel lamellae of the type we model but with a growth twinned relationship between neighboring bands. These twinned lamellae would share their [112] and [$11\bar{1}$] directions but not [110]. Since the exact microstructure of the specimen—in particular, the volume fraction of a lamella vs. its twin—was not reported, we are unable to attempt the analysis of the laminate. However, there are strong indications from previous work (James and Kinderlehrer, 1993) that a slab of growth twinned material will behave similar to the single lamella.

The curves of Fig. 7 clearly show the existence of an intermediate regime between the initial and the final, saturated, configuration, at field strengths just exceeding 250 Oe. In this intermediate regime, the magnetization in parts of the specimen rotates out of the plane generated by the [112] and [$1\ 1\ \bar{1}$] directions, as it can be seen from Table 1. This may explain a striking feature of the experimental curves of Fig. 7, namely, that the steep rise in the $11\bar{1}$ curve occurs earlier than the rise in the 112 curve, even though the field was applied along 112. Indeed, the transition from the initial state $(\boldsymbol{E}_4, \pm\boldsymbol{m}_4)$ to, say, $(\boldsymbol{E}_3, \boldsymbol{m}_3)$ is accompanied by large strain changes along [$11\bar{1}$], and small strain changes along [112]. The further transition to $(\boldsymbol{E}_1, \boldsymbol{m}_1)$ (the closest we can get to a saturated state along [112] within our model) determines significant [112] strain changes, but no changes of length along [$11\bar{1}$].

Acknowledgements

Part of this research was conducted while ADS was enjoying the hospitality of the Department of Aerospace Engineering and Mechanics at the University of Minnesota as a Visiting Professor for Research. Fruitful discussions with S. Müller are gratefully acknowledged. The authors would also like to thank ONR (N00014-99-1-0925 and N00014-95-1-1145), AFOSR/MURI (F49620-98-1-0433), ARO (DAAG55-98-1-0335) and NSF (DMS-0074043) for supporting this work.

Appendix A.

A.1. Ellipsoids

Ellipsoids have the property that a uniform state minimizes the magnetostatic energy among all magnetization states with prescribed average. In addition, such a uniform magnetic state generates a magnetic field which is uniform in the interior of the ellipsoid. Thus, in view of the linearity of the relation between magnetization and induced magnetic field, for a given ellipsoid Ω there exists a symmetric matrix $\boldsymbol{D}$ such that $-4\pi\boldsymbol{Dm}$ is the magnetic field induced in the interior of Ω by the uniform magnetization $\boldsymbol{m}$ (For $\boldsymbol{m}$ measured in emu/cm^3, $-4\pi\boldsymbol{Dm}$ gives the induced magnetic field measured in Oe). The matrix $\boldsymbol{D}$ is called demagnetizing matrix, and it has unit trace.

Lemma A.1. *Let Ω be an ellipsoid, $|\Omega|$ its volume, and $\boldsymbol{D}$ its demagnetizing matrix. Given a vector $\boldsymbol{m}^\circ$, let*

$$\mathscr{M}_\circ = \{\boldsymbol{m} \in L^2(\mathbb{R}^3, \mathbb{R}^3)\colon \langle \boldsymbol{m} \rangle = \boldsymbol{m}^\circ, \boldsymbol{m} = 0 \text{ outside } \Omega\}$$

be magnetizations with average $\boldsymbol{m}^\circ$. Then, denoting by $\zeta_{\boldsymbol{m}}$ the solution of $\operatorname{div}(-\nabla\zeta + 4\pi\boldsymbol{m}) = 0$ *corresponding to $\boldsymbol{m} \in \mathscr{M}_\circ$, we have*

$$\min_{\mathscr{M}_\circ} \frac{1}{8\pi} \int_{\mathbb{R}^3} |\nabla\zeta_{\boldsymbol{m}}(\boldsymbol{x})|^2 \mathrm{d}\boldsymbol{x} = 2\pi|\Omega|\boldsymbol{m}^\circ \cdot \boldsymbol{Dm}^\circ$$

Proof. By adding and subtracting $\nabla\zeta_\circ := \nabla\zeta_{\chi_\Omega \boldsymbol{m}^\circ}$, we have

$$\begin{aligned}
\int_{\mathbb{R}^3} |\nabla\zeta_{\boldsymbol{m}}|^2 &= \int_{\mathbb{R}^3} \{|\nabla(\zeta_{\boldsymbol{m}} - \zeta_\circ)|^2 + 2\nabla(\zeta_{\boldsymbol{m}} - \zeta_\circ)\cdot\nabla\zeta_\circ + |\nabla\zeta_\circ|^2\} \\
&= \int_{\mathbb{R}^3} \{|\nabla(\zeta_{\boldsymbol{m}} - \zeta_\circ)|^2 + |\nabla\zeta_\circ|^2\} + 2(4\pi)^2\boldsymbol{Dm}^\circ \cdot \int_\Omega \{\boldsymbol{m} - \boldsymbol{m}^\circ\} \\
&= \int_{\mathbb{R}^3} \{|\nabla(\zeta_{\boldsymbol{m}} - \zeta_\circ)|^2 + |\nabla\zeta_\circ|^2\} \\
&\geqslant \int_{\mathbb{R}^3} |\nabla\zeta_\circ|^2,
\end{aligned}$$

where we have used the fact that, on Ω, $\nabla\zeta_\circ = 4\pi \boldsymbol{D}\boldsymbol{m}^\circ$ is constant, together with the identity $\operatorname{div}(-\nabla(\zeta_{\boldsymbol{m}} - \zeta_\circ) + 4\pi(\boldsymbol{m} - \boldsymbol{m}^\circ)\chi_\Omega) = 0$ in its weak form

$$\int_{\mathbb{R}^3} \nabla(\zeta_{\boldsymbol{m}} - \zeta_\circ) \cdot \nabla\zeta_\circ \,\mathrm{d}\boldsymbol{x} = 4\pi \int_\Omega (\boldsymbol{m} - \boldsymbol{m}^\circ) \cdot \nabla\zeta_\circ \,\mathrm{d}\boldsymbol{x}.$$

The result then follows from Eq. (2.10) evaluated at $\boldsymbol{m} = \boldsymbol{m}^\circ\chi_\Omega$. $\square$

A.2. Basic facts about weak convergence and Young measures

In this section, we present in an informal way the few basic facts about weak covergence and Young measures which are used in the paper. The interested reader is referred to Ball (1990), Dacorogna (1989), Evans (1990), Müller (1998) and Tartar (1979) for a more rigorous and comprehensive exposition.

From every bounded sequence $f^{(k)} \in L^2(\Omega)$ with values in $\mathbb{R}^{\mathrm{m}}$ one can extract a subsequence, not relabelled, [3] which converges weakly in L^2 to some $f \in L^2(\Omega)$, i.e.

$$\lim_k \int_\Omega f^{(k)}(\boldsymbol{x})\phi(\boldsymbol{x})\,\mathrm{d}\boldsymbol{x} = \int_\Omega f(\boldsymbol{x})\phi(\boldsymbol{x})\,\mathrm{d}\boldsymbol{x} \quad \forall \phi \in L^2(\Omega) \tag{A.1}$$

denoted with $f^{(k)} \rightharpoonup f$. This sequence generates a Young measure $\nu_{\boldsymbol{x}}$ if the following holds

$$\lim_k \int_\Omega F(f^{(k)}(\boldsymbol{x}))\phi(\boldsymbol{x})\,\mathrm{d}\boldsymbol{x} = \int_\Omega \int_{\mathbb{R}^{\mathrm{m}}} F(g)\phi(\boldsymbol{x})\,\mathrm{d}\nu_{\boldsymbol{x}}(g)\,\mathrm{d}\boldsymbol{x} \quad \forall \phi \in L^1(\Omega) \tag{A.2}$$

for every continuous function $F \in C^0(\mathbb{R}^{\mathrm{m}})$ that grows quadratically at infinity. The weak limit $f(\boldsymbol{x})$ of $f^{(k)}$ identifies the limit local averages of $f^{(k)}$ around each point $\boldsymbol{x} \in \Omega$. To see this, take as test function ϕ in (A.1) the characteristic function of a small ball around $\boldsymbol{x}$. The Young measure $\nu_{\boldsymbol{x}}$ is a probability measure (i.e., nonnegative and with total mass equal to one) which identifies the weak limits of all continuous functions of $f^{(k)}$, hence it contains more information on the asymptotic properties of $f^{(k)}$ than its weak limit. In fact, the weak limit f is the center of mass of $\nu_{\boldsymbol{x}}$:

$$f(\boldsymbol{x}) = \int_{\mathbb{R}^{\mathrm{m}}} g\,\mathrm{d}\nu_{\boldsymbol{x}}(g). \tag{A.3}$$

The Young measure $\nu_{\boldsymbol{x}}$ of $f^{(k)}$ contains also information about the asymptotic distribution of the values taken by $f^{(k)}$ in a neighborhood of each point $\boldsymbol{x}$. These values constitute the subset of $\mathbb{R}^{\mathrm{m}}$ where $\nu_{\boldsymbol{x}}$ is positive, i.e., the support of $\nu_{\boldsymbol{x}}$ denoted by $\operatorname{supp}\nu_{\boldsymbol{x}}$. We will be mostly concerned with the case in which $\operatorname{supp}\nu_{\boldsymbol{x}}$ is discrete

$$\operatorname{supp}\nu_{\boldsymbol{x}} \subset \{g_1, \ldots, g_n\}.$$

In this case $\nu_{\boldsymbol{x}}$ is a convex combination of Dirac masses

$$\nu_{\boldsymbol{x}} = \sum_{i=1}^n \lambda_i(\boldsymbol{x})\delta_{g_i},$$

[3] Here and in the rest of the paper, we assume that a convergent subsequence is extracted from a given one, but not relabelled, whenever this is necessary to give a meaning to taking the limit of the given sequence.

where δ_{g_i} is a Dirac mass at g_i and $\sum_{i=1}^n \lambda_i(\boldsymbol{x}) = 1$ almost everywhere in Ω. Moreover, Eqs. (A.3) and (A.2) reduce to

$$f(\boldsymbol{x}) = \sum_{i=1}^{n} \lambda_i(\boldsymbol{x}) g_i$$

and

$$\lim_k \int_\Omega F(f^{(k)}(\boldsymbol{x}))\,\mathrm{d}\boldsymbol{x} = \sum_{i=1}^{n} F(g_i) \int_\Omega \lambda_i(\boldsymbol{x})\,\mathrm{d}\boldsymbol{x}.$$

Our reason to use Young measures in this paper is precisely the following. A formal way of saying that a sequence of pairs $(\boldsymbol{E}^{(k)}(\boldsymbol{x}), \boldsymbol{m}^{(k)}(\boldsymbol{x}))$ in $\mathscr{A}$ takes values near the wells $\mathbb{K}$ except on sets that contribute negligibly to the energy (transition layers) is to say that the support of the Young measure $v_{\boldsymbol{x}}$ of $(\boldsymbol{E}^{(k)}(\boldsymbol{x}), \boldsymbol{m}^{(k)}(\boldsymbol{x}))$ is contained in $\mathbb{K}$: briefly, $\operatorname{supp} v_{\boldsymbol{x}} \subset \mathbb{K}$. More precisely, let $(\boldsymbol{E}^{(k)}(\boldsymbol{x}), \boldsymbol{m}^{(k)}(\boldsymbol{x}))$ be bounded in $L^2(\Omega)$ and let $v_{\boldsymbol{x}}$ be the corresponding Young measure . Let $\Psi(\boldsymbol{E}, \boldsymbol{m}) \geqslant 0$ be any continuous function of strain-magnetization that vanishes exactly on $\mathbb{K}$ and that grows quadratically to infinity as $|\boldsymbol{E}|, |\boldsymbol{m}|$ tend to infinity. Then $\operatorname{supp} v_{\boldsymbol{x}} \subset \mathbb{K}$ is equivalent to the statement

$$\int_\Omega \Psi(\boldsymbol{E}^{(k)}(\boldsymbol{x}), \boldsymbol{m}^{(k)}(\boldsymbol{x}))\,\mathrm{d}\boldsymbol{x} \to 0 \text{ as } k \to \infty. \tag{A.4}$$

Throughout the paper, the statement $\operatorname{supp} v_{\boldsymbol{x}} \subset \mathbb{K}$ for a sequence $(\boldsymbol{E}^{(k)}, \boldsymbol{m}^{(k)})$ can be taken to mean precisely (A.4) for any Ψ having the given properties. In particular, setting $\Phi = \Psi$ in (A.4), we see that for a sequence whose Young is supported on the energy wells, the contribution to the total anisotropy energy, which is localized on the transition layers, vanishes as k tends to infinity.

A.3. A result on the 'excess' energy

In the proof of Theorem 4.1 we have used Lemma A.2 below which states an important localization property of the 'excess' contribution to the magnetostatic energy (the one due to internal poles). This is a direct consequence of a corresponding localization property of H-measures (Tartar, 1990), but we give here a direct proof for the reader's convenience.

Lemma A.2. *Let $\boldsymbol{m}^{(k)} \in \mathscr{M}$ be a sequence of magnetizations such that $\boldsymbol{m}^{(k)} \rightharpoonup 0$ in $L^2(\mathbb{R}^3, \mathbb{R}^3)$, and*

$$\nabla \zeta_{\chi_\Omega \boldsymbol{m}^{(k)}} \to 0 \quad \text{in } L^2(\mathbb{R}^3, \mathbb{R}^3).$$

Then, for every measurable $\Omega' \subset \Omega$,

$$\nabla \zeta_{\chi_{\Omega'} \boldsymbol{m}^k} \to 0 \quad \text{in } L^2(\mathbb{R}^3, \mathbb{R}^3).$$

Proof. Let's denote $\boldsymbol{m}^k$ by f^k and $\nabla \zeta_f$ by Pf. We have to show that if

$$f^k \rightharpoonup 0, \text{ and } Pf^k \to 0 \quad \text{in } L^2(\mathbb{R}^3, \mathbb{R}^3) \tag{A.5}$$

then

$$P(\phi f^k) \to 0 \quad \text{in } L^2(\mathbb{R}^3, \mathbb{R}^3), \tag{A.6}$$

where ϕ is the characteristic function of an arbitrary measurable subset Ω' of Ω. We will make use (without proof) of the following estimates, in which $g \in L^2(\mathbb{R}^3, \mathbb{R}^3)$, $\operatorname{div} g \in L^2(\mathbb{R}^3)$, and g has compact support. They follow directly from the Fourier transform and from the Green function representations of the linear operator P.

$$||Pg||_{L^2} \leqslant 4\pi ||g||_{L^2}, \tag{A.7}$$

$$||\nabla Pg||_{L^2} \leqslant 4\pi ||\operatorname{div} g||_{L^2}, \tag{A.8}$$

$$|Pg(\boldsymbol{x})| \leqslant \frac{C}{|\boldsymbol{x}|^3} ||g||_{L'}, \quad |\boldsymbol{x}| \geqslant 2 \operatorname{diam} (\operatorname{supp} g), \tag{A.9}$$

where diam $(\operatorname{supp} g)$ is the (maximum) diameter of the support of g, $\operatorname{supp} g$. We first show that Eq. (A.6) holds for $\phi \in C_0^\infty(\mathbb{R}^3)$. It follows, respectively, from Eq. (A.5), the identity $\operatorname{div}(f - Pf) = 0$, and the fact that ϕ has compact support, that

$$\phi(f^k - Pf^k) \rightharpoonup 0 \quad \text{in } L^2(\mathbb{R}^3, \mathbb{R}^3) \tag{A.10}$$

$$\operatorname{div}(\phi(f^k - Pf^k)) = \nabla\phi \cdot (f^k - Pf^k) \rightharpoonup 0 \quad \text{in } L^2(\mathbb{R}^3) \tag{A.11}$$

$$\operatorname{supp} \phi(f^k - Pf^k) \subset \operatorname{supp} \phi. \tag{A.12}$$

Thus we can set $g^k = \phi(f^k - Pf^k)$ in Eqs. (A.7), (A.8), (A.9) and, in addition, we have that $||g^k||_{L^2}$ and $||\operatorname{div} g^k||_{L^2}$ are bounded. It follows that Pg^k is bounded in $W^{1,2}$ and precompact in L^2, so that

$$Pg^k \to 0 \quad \text{in } L^2(\mathbb{R}^3, \mathbb{R}^3)$$

and in turn, since $Pf^k \to 0$ by Eq. (A.5), that

$$P(\phi f^k) \to 0 \quad \text{in } L^2(\mathbb{R}^3, \mathbb{R}^3) \quad \forall \phi \in C_0^\infty(\mathbb{R}^3). \tag{A.13}$$

References

Ball, J.M., 1990. A version of the fundamental theorem for Young measures. In: Rascle, M., Serre, D., Slemrod, M. (Eds.), PDE's and Continuum Models of Phase Transitions, Springer Lecture Notes in Physics, Vol. 359. Springer, Berlin.

Ball, J.M., Chu, C., James, R.D., 1995. Hysteresis during stress-induced variant rearrangement. J. Phys. IV, Colloque C8 (5), 245–251.

Ball, J.M., James, R.D., 1992. Proposed experimental tests of a theory of fine microstructure and the two-well problem. Phil. Trans. R. Soc. London A 228, 389–450.

Bhattacharya, K., 1993. Comparison of geometrically nonlinear and linear theories of martensitic transformation. Continuum Mech. Thermodyn. 5, 205–242.

Bhattacharya, K., 2000. Personal communication.

Brown, W.F., 1963. Micromagnetics. Wiley, New York.

Brown, W.F., 1966. Magnetoelastic Interactions. Springer, Berlin.

Clark, A.E., 1992. High power rare earth magnetostrictive materials. In: Rogers, C.A., Rogers, R.C. (Eds.), Recent Advances in Adaptive and Sensory materials. Technomic: Lancaster, Basel.

Cui, J., James, R.D., 2000. Study of Fe_3Pd and related alloys for ferromagnetic shape memory. J. Appl. Phys., accepted.
Dacorogna, B., 1989. Direct Methods in the Calculus of Variations. Springer, Berlin.
De Simone, A., 1993. Energy minimizers for large ferromagnetic bodies. Arch. Rat. Mech. Anal. 125, 99–143.
DeSimone, A., 1994. Magnetostricitve solids: macroscopic response and microstructure evolution under applied magnetic fields and loads. J. Intell. Mater. Systems Struct. 5, 787–794.
DeSimone, A., 1996. Characterization of the macroscopic response of magnetostrictive materials via microstructural analysis. ZAMM 76 (S2), 397–400.
De Simone, A., James, R.D., 1997. A theory of magnetostriction oriented towards applications. J. Appl. Phys. 81 (8), 5706–5708.
Evans, L.C., 1990. Weak Convergence Methods for Nonlinear Partial Differential Equations. American Mathematical Society, Providence, RI.
James, R.D., Hane, K.F., 2000. Martensitic transformations and shape memory materials. Acta Mater. 48, 197–222.
James, R.D., Kinderlehrer, D., 1993. Theory of magnetostriction with applications to $Tb_xDy_{1-x}Fe_2$. Philos. Mag. B 68, 237–274.
James, R.D., Müller, S., 1994. Internal variables and fine-scale oscillations in micromagnetics. Continuum Mech. Thermodyn. 6, 291–336.
James, R.D., Wuttig, M., 1996. Alternative smart materials, In: Varadan, V.V., Chandra, J. (Eds.), SPIE Proceedings, Vol. 2715, pp. 420–426.
James, R.D., Wuttig, M., 1998. Magnetostriction of martensite. Philos. Mag. A 77, 1273–1299.
Landau, L.D., Lifschitz, E.M., 1935. On the theory of the dispersion of magnetic permeability in ferromagnetic bodies. Phys. Z. Sow 8, 153–169.
Müller, S. Variational models for microstructure and phase transitions. MPI for Mathematics in the Sciences, Lecture Notes 2/1998, http://www.mis.mpg.de/cgi-bin/lecturenotes.pl
Pedregal, P., 1994. Relaxation in ferromagnetism: the rigid case. J. Nonlinear Sci. 4, 105–125.
Qi Pan, James, R.D., 2000. Micromagnetic study of Ni_2MnGa under applied field (invited). J Appl. Phys. 87, 4702–4706.
Rogers, R.C., 1991. A nonlocal model for the exchange energy in ferromagnetic materials. J. Int. Eq. Appl. 33, 85–127.
Tartar, L., 1979. Compensated compactness and partial differential equations. In: Knops, R. (Ed.), Nonlinear Analysis and Mechanics: Heriot-Watt Symposium. Vol. IV. Pitman, London.
Tartar, L., 1990. H-measures: a new approach for studying homogenisation, oscillations and concentration effects in partial differential equations. Proc. Roy. Soc. Edin. 115A, 193–230.
Tartar, L., 1995. Beyond Young measures. Meccanica 30, 505–526.
Teter, J.P., Wun-Fogle, M., Clark, A.E., Mahoney, K., 1990. Anisotropic perpendicular axis magnetostriction in twinned $Tb_xDy_{1-x}Fe_{1.95}$. J. Appl. Phys. 67 (9), 5004–5006.
Tickle, R., James, R.D., 1999. Magnetic and magneto-mechanical properties of Ni_2MnGa. J. Magn. Magn. Mater. 195, 627–638.
Tickle, R., James, R.D., Shield, T., Wuttig, M., Kokorin, V.V., 1999. Ferromagnetic shape memory in the NiMnGa system. IEEE Trans. Magn. 35, 4301–4310.
Ullakko, K., Huang, J.K., Kantner, C., O'Handley, R.C., Kokorin, V.V., 1996. Large magnetic-field-induced strains in Ni_2MnGa single crystals. Appl. Phys. Lett. 69 (13), 1966–1968.